Geolocation Assessment/validation Methods for EPS-SG ICI and MWI (GAMES)

Final meeting – 26 Jan. 2021

F.S. Marzano, M. Papa, N. Pierdicca (SUR-CRAS)
M. Montopoli, D. Casella, G. Panegrossi (CNR-ISAC)
B. Rydberg, J. Moller (Molflow)

Contacts: frank.marzano@uniroma1.it

SAPIENZA Università di Roma
Consiglio Nazionale delle Ricerche
Istituto di Scienze della Atmosfera e del Clima
Molflow

Outline

- **GAMES project**
- **GAMES rationale and objectives**
- **Task 1. Landmark target methodology**
  - Searching for ICI surface landmark targets
  - Results of ICI geolocation assessment
- **Task 2. Atmospheric target approach**
  - ICI absolute geolocation using DCC and WVM
  - ICI relative geolocation using BG approach
- **Task 3. Geolocation algorithm implementation**
- **Conclusion**

GAMES project team

GAMES consortium

SAPIENZA
UNIVERSITÀ DI ROMA

F.S. Marzano, M. Papa

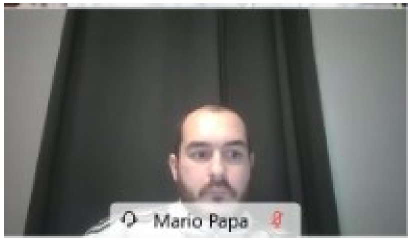

Roma, IT

Consiglio Nazionale delle Ricerche
ISAC
Istituto di Scienze della Atmosfera e del Clima

M. Montopoli, D. Casella

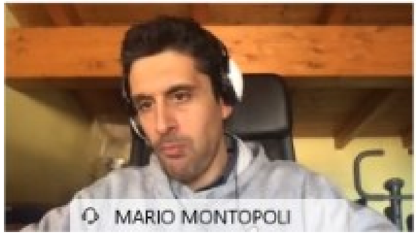

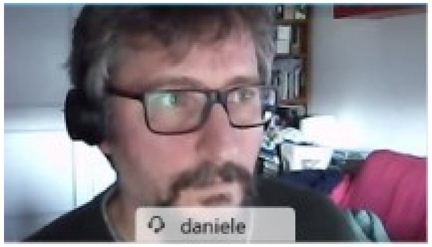

Roma, IT

MolFloW

B. Rydberg

Gråbo, SW

EUMETSAT

Project officer
V. Mattioli

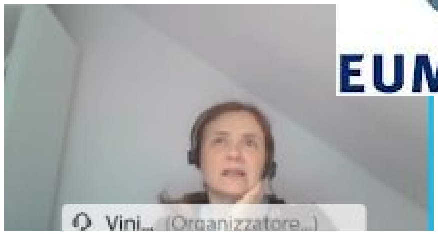

GAMES work breakdown structure

GAMES

Geolocation Assessment Methods for EPS SG ICI and MWI

Task	Work package	WPR
Task 0	WP 0: Management	WPR: Frank Silvio Marzano, SUR-CRAS
Task 1	WP 1: Landmark target assessment method	WPR: Mario Papa, SUR-CRAS
Task 2	WP 2: Atmospheric target assessment methods	WPR: Mario Montopoli, CNR-ISAC
Task 3	WP 3: Assement method implementation	WPR: Bengt Rydberg, Molflow

In response to EUMETSAT ITT n. 19/218140 on the "*Development of Geolocation Validation Methods for EPS-SG ICI and MWI*".

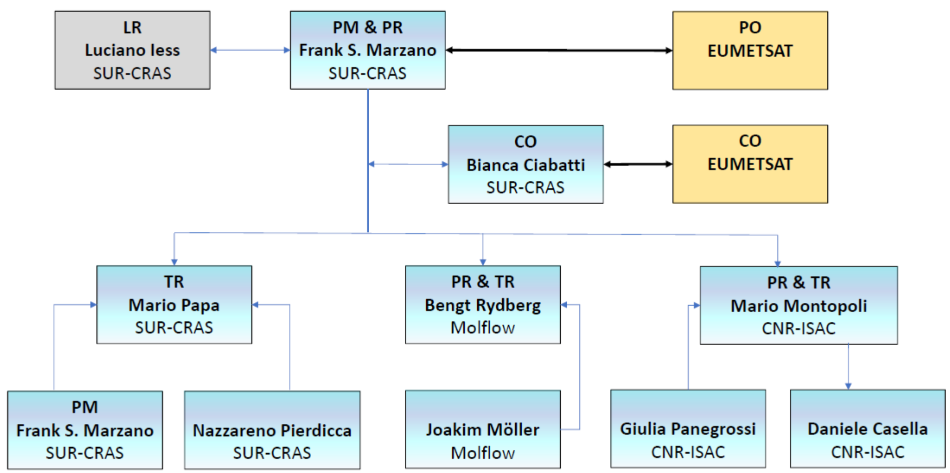

GAMES project timeline

GAMES Time schedule together main deliverables and meetings

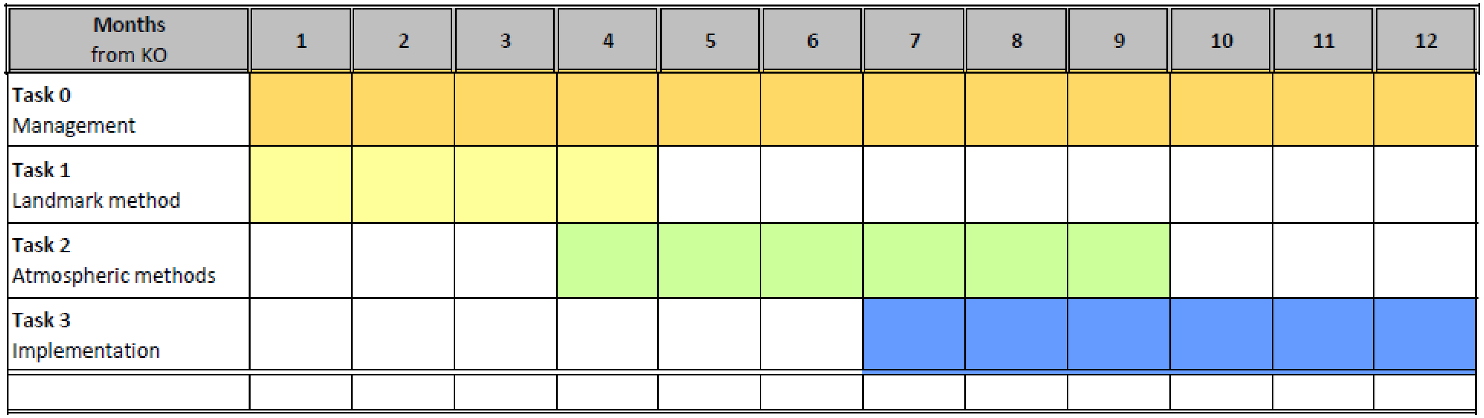

	1	2	3	4	5	6	7	8	9	10	11	12
MEETINGS	KOM			PM1		MTR			PM2			FRM
MILESTONES				MS1					MS2			MS3
DELIVERABLES	D01			D04=T1R		D05=T2P			D06=T2D	D07=T2R	D08-09-10	D11-12-13
		D02a	D02b		D02c	D02d	D02e	D02f	D02g		D02h	
			D03a			D03b			D03c			
											ATBDv1	ATBDv2

LEGEND:

ATBD	Algorithm Theoretical Basis Document
DXX	Deliverable XX
DXXy	Deliverable XX on y-basis (monthly or three-monthly)
FRM	Final Review Meeting (Darmstadt, D)
KOM	Kick Off Meeting (Darmstadt, D)
MTR	Mid Term Review (Rome, I)
PM1, PM2	Progress Meeting 1, 2 (telecon)
PPM, MTM, FDM	Pre-Payment, Mid-Term, Final-Term Milestone
T1R	Task 1 Report
T2R, T2P, T2D	Task 2 Report, Preliminary, Draft
MS1, MS2, MS3	MilestoneTask1, MilestoneTask2, Final MileStone

Actual meeting plan

- KOM on 04.09.2019
- MTR on 06.06.2020
- FTM on 26.01.2021
- 6 progress meetings

Outline

- **GAMES project**
- **GAMES rationale and objectives**
- **Task 1: Landmark target methodology**
  - Searching for ICI surface landmark targets
  - Results of ICI geolocation assessment
- **Task 2: Atmospheric target approach**
  - ICI absolute geolocation using DCC and WVM
  - ICI relative geolocation using BG approach
- **Task 3: Geolocation algorithm implementation**
- **Conclusion**

Ice Cloud Imager (ICI) on board EPS-SG

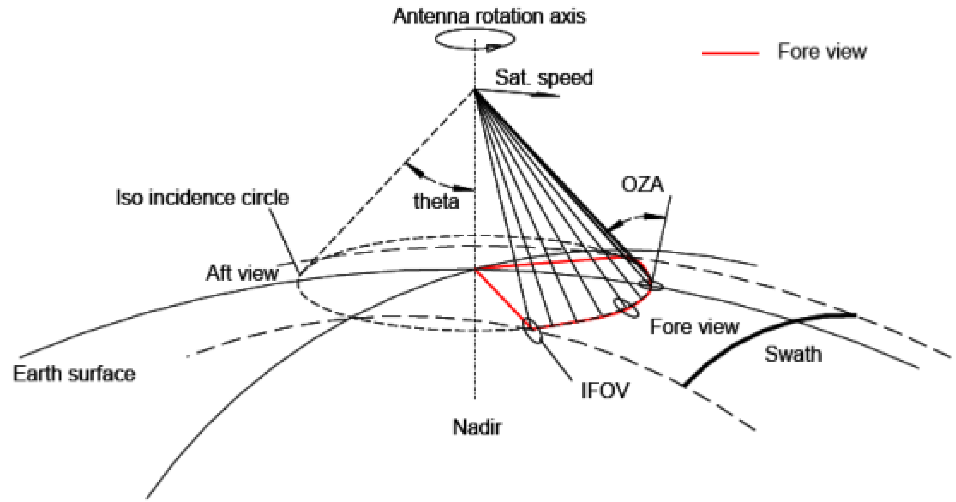

Ice Cloud Imager (ICI)

- EUMETSAT sub-millimetre-wave conically-scanning (at 53°±2°) radiometric imager with a swath of 1700 km
- Flying at 817 km on board the EPS-SG (EUMETSAT Polar System - Second Generation) satellite B mission
- Launch foreseen in 2024.

Channel	Frequency (GHz)	NEΔT (K)	Polarisation	Footprint Size at 3dB (km)
ICI-1	183.31±7.0	0.8	V	16
ICI-2	183.31±3.4	0.8	V	16
ICI-3	183.31±2.0	0.8	V	16
ICI-4	243.2±2.5	0.7	V, H	16
ICI-5	325.15±9.5	1.2	V	16
ICI-6	325.15±3.5	1.3	V	16
ICI-7	325.15±1.5	1.5	V	16
ICI-8	448±7.2	14	V	16
ICI-9	448±3.0	1.6	V	16
ICI-10	448±1.4	2.0	V	16
ICI-11	664±4.2	1.6	V, H	16

Goals of ICI and geolocation issue

The **primary objective** of the Ice Cloud Imaging (ICI) mission is to:

- **retrieve ice clouds**, especially cirrus clouds, cloud ice water path, cloud ice effective radius and cloud altitude, providing vertical **humidity profile** and vertical profiles of **hydrometeors** (cloud ice, graupel and snow)
- **validate ice clouds** in **weather and climate** models through the provision of ice cloud products, including bulk microphysical variables
- **estimate snowfall** distributions in support of numerical weather **prediction and nowcasting**.

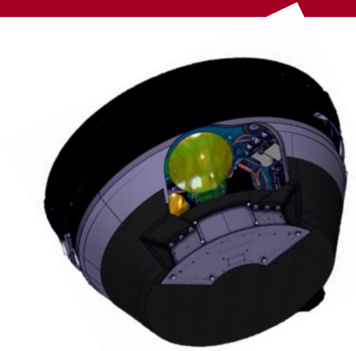

But, how to validate the geolocation of ICI imagery?

Open issues on ICI geolocation

MW imager conventional geolocation approach:
- Use low frequency channels (19, 37 or 89 GHz)
- Cross-correlate with natural target contours such as coastlines
- Heritage of SSMI, SSMIS, AMSU

F17 SSMIS 19 GHz V (2016/07/24)

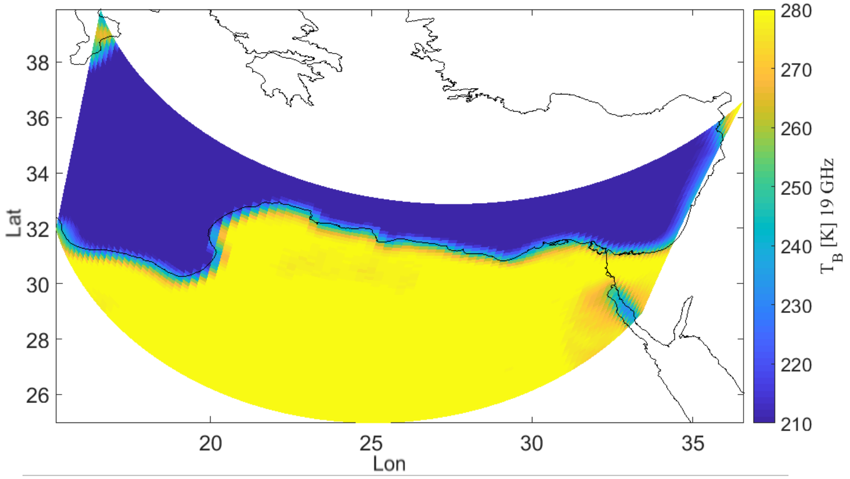

High coastline contrast for SSMIS at 19 GHz V

ICI geolocation issues

At frequencies ≥ 183 GHz coastline contrast decreases because:
- water body emissivity increases
- atmospheric transmittance reduces

with frequency

F17 SSMIS 183 ±7 GHz H (2016/07/24)

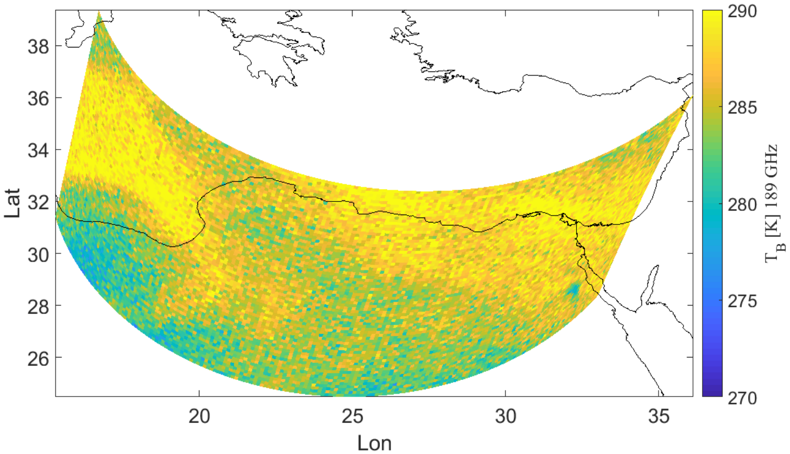

Poor coastlines contrast for SSMIS at 183 ±7 GHz H

Goals of GAMES project

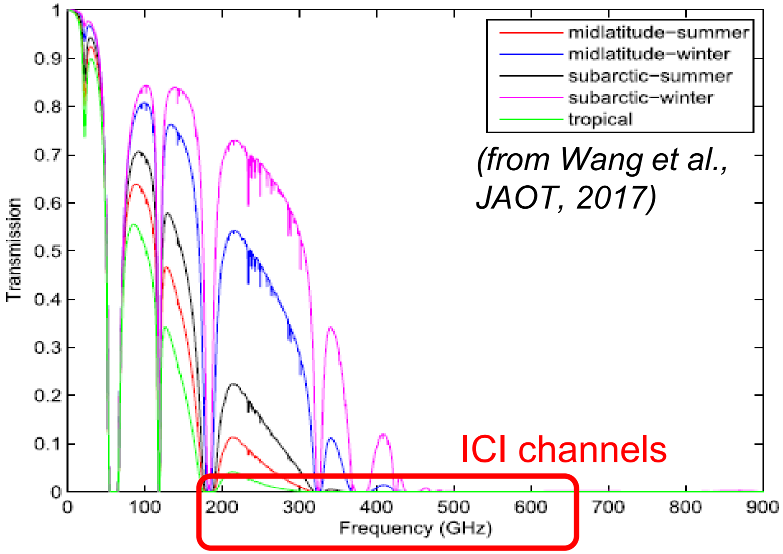

Open questions:

1. Can we geolocate ICI at 183 and 243 GHz using surface landmarks?
2. How can we approach the geolocation of ICI higher frequency channels around 325, 448 and 664 GHz?

The **goals** of GAMES:

1. Consider **lower-frequency** channels of ICI, e.g. 183.31±7.0 and 243.2±2.5, and search for **landmark targets** using reference contour sources
2. Explore the possibility to identify **atmospheric targets** using Meteosat IR images as reference contour sources
3. Investigate **relative geolocation** assessment for ICI higher frequency wrt lower frequency ones
4. Implement a **GAMES tool** for ICI selecting assessed approaches useful for the ICI commissioning phase

Block diagram of GAMES approach

Target contour matching (TCM) – Landmark and Atmospheric targets

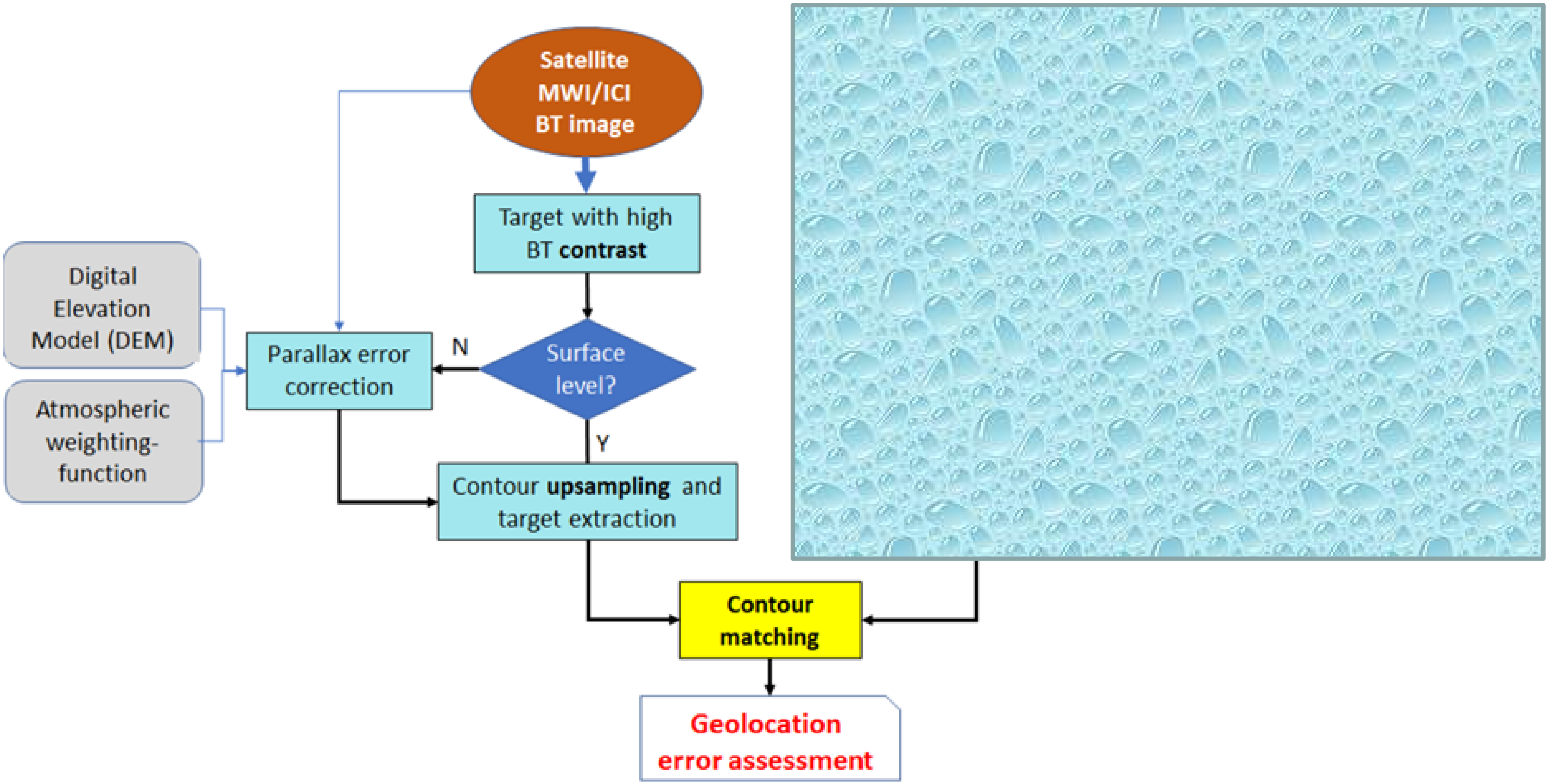

Note – Rayleigh-Jeans or Planck law?

Since ICI provides channel frequencies up to 664 GHz and the **Rayleigh-Jeans approximation of the Planck function is not necessarily valid**. However, we can generalize the spectral brightness temperature T_{Bf}, by inverting the Planck law for the spectral brightness B_f

$$T_{Bf} = \frac{hf}{k} ln^{-1}\left(\frac{2hf^3}{c^2 B_f} + 1\right)$$

which reduces to the Rayleigh-Jeans approximation T_{BfRJ} at low frequencies

$$T_{Bf} \simeq \frac{c^2}{2kf^2} B_f \doteq T_{BfRJ}$$

*The **percentage error**, defined as $\varepsilon_{\%RJ}=100(T_{BfRJ} - T_{Bf})/T_{Bf}$ and due to the Rayleigh-Jeans hypothesis, is shown for values of T_{Bf} between 190 K and 270 K and for a frequency interval between 5 and 700 GHz. The ICI frequencies are also highlighted by vertical bars.*

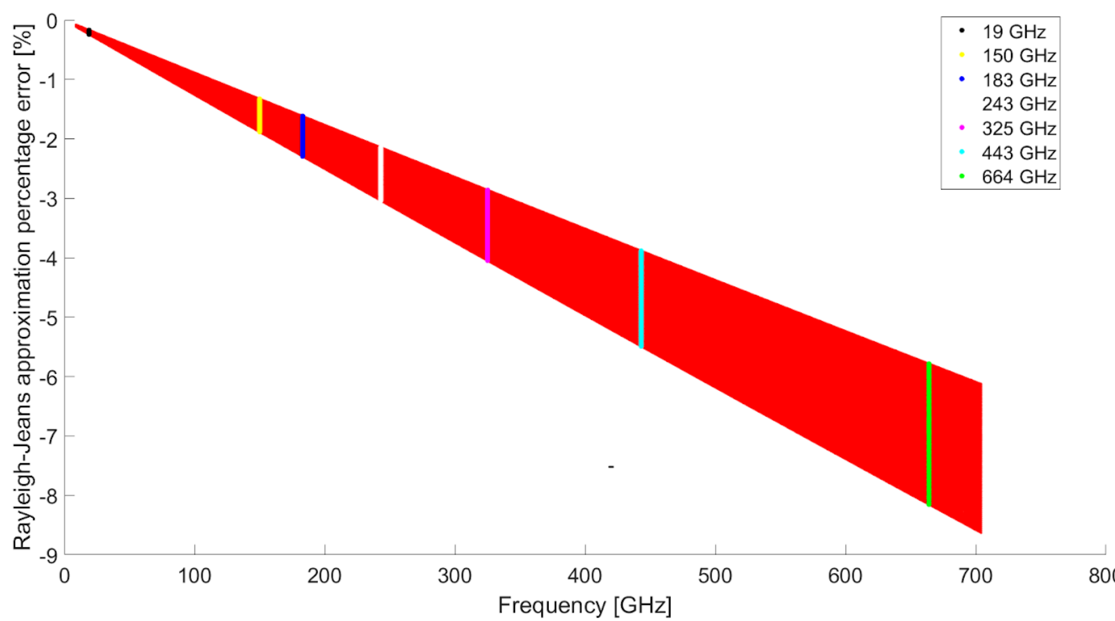

Outline

- **GAMES project**
- **GAMES rationale and objectives**
- **Task 1. Landmark target methodology**
  - Searching for ICI surface landmark targets
  - Results of ICI geolocation assessment
- **Task 2. Atmospheric target approach**
  - ICI absolute geolocation using water vapor gradients
  - ICI relative geolocation using Backus-Gilbert approach
- **Task 3. Geolocation algorithm implementation**
- **Conclusion**

Task 1. Looking for landmarks on the Earth …

Wallpops, 2019

Task 1. Radiative transfer background

Assuming a homogeneous absorbing isothermal (constant temperature and interaction parameters) **small-albedo layer** of thickness H:

$$\boxed{T_B = e_s\, T_S\, e^{-k_e L} + (1-w)\, T_0\, [1 - e^{-k_e L}]}$$

- e_s : surface emissivity (adim.)
- T_S : surface temperature(K)
- $T_0 = T(z)$ constant atmospheric temperature (K)
- k_e : atmospheric extinction coefficient (km^{-1})
- w :atmospheric albedo (adim.)
- L : atmospheric slant path ($H = L\, cos\theta$ with θ the nadir angle) (km)
- $e^{-k_e L} = t(L)$: atmospheric transmittance (adim.)

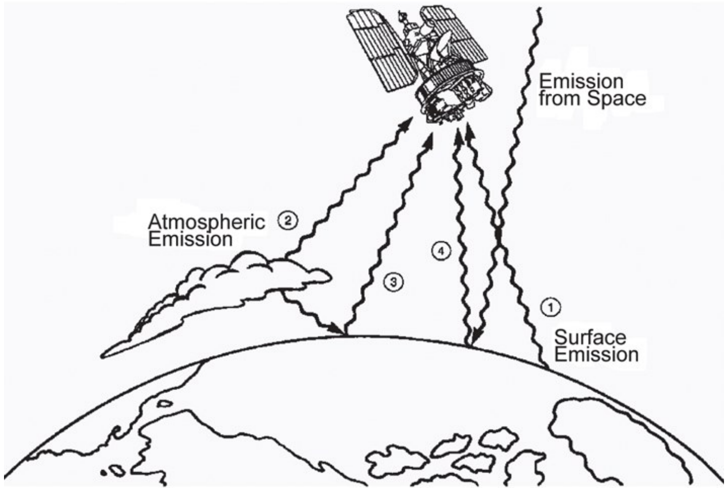

Clear-air

Pixel 1

$$T_{B_1} = e_{s_1}\, T_{S_1}\, e^{-k_e L} + (1-w)\, T_0\, [1 - e^{-k_e L}]$$

Pixel 2

$$T_{B_2} = e_{s_2}\, T_{S_2}\, e^{-k_e L} + (1-w)\, T_0\, [1 - e^{-k_e L}]$$

$$\boxed{\Delta T_B = t(L)\, [e_{s_1}\, T_{S_1} - e_{s_2}\, T_{S_2}]}$$

Brightness temperature contrast

Task 1. Landmark target research criteria

GENERAL CRITERIA

- Criterion 1: landmark feature with a high surface BT contrast (**discriminability**)
- Criterion 2: period/region with a low atmospheric transmittance (**visibility**)
- Criterion 3: covering the whole year as a full set (**flexibility**)

- High-latitude coastlines (Artic/Antartic?)
- High-altitude water bodies (Lakes?)
- High-slope mountains (Andes, Himalaya?)

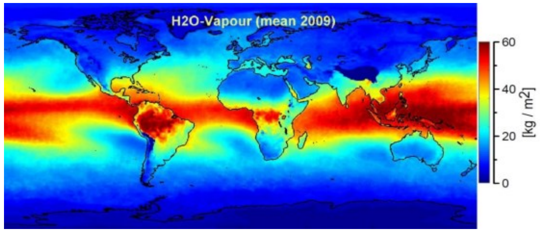

(http://www.globvapour.info/newsarchive.html)

Southern Hemisphere (SH)

(visible from April to September)

- Antarctic ice shelves (Antarctica)
  - Ross
  - Filchner-Ronne
  - Amery
- Titicaca lake (Peru-Bolivia)
- Andean mountains (Chile-Peru)

Northern Hemisphere (NH)

(visible from October to March)

- Qinghai lake (Inland China)
- Karakorum mountains (Himalaya)
- Nares Strait (North Greenland)
- Hudson's Bay (Eastern Canada)

Task 1. Simulate using SSMIS imagery at 183.31±6.6

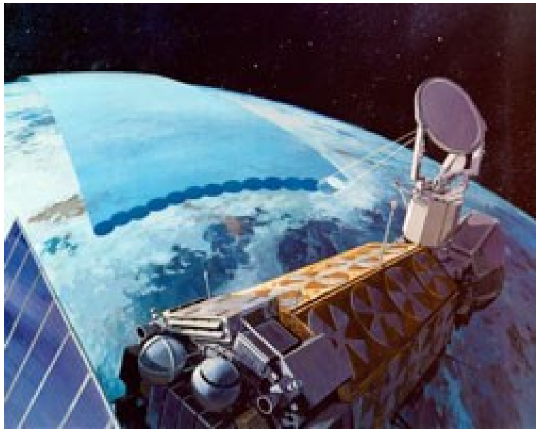

Special Sensor Microwave Imager/Sounder (SSMIS)

- Passive conically scanning microwave radiometer
- 24-channel, 21-frequency, linearly polarized passive microwave radiometer system.
- On board the USAF Defense Meteorological Satellite Program (DMSP) F-16, F-17, F-18 and F-19 satellites

Radiometric characteristics of the SSMIS (H: horizontal; V: vertical; RC: right circular).

Frequency (GHz)	Polarization (V, H, and RC)	Along-track resolution (km)	Cross-track resolution (km)	Spatial sampling (km× km)	Instrument noise (K)
19.35	H, V	73	47	45 × 74	0.35
22.235	V	73	47	45 × 74	0.45
37.0	H, V	41	31	28 × 45	0.22
50.3	H	17.6	27.3	37.5 × 37.5	0.34
52.8	H	17.6	27.3	37.5 × 37.5	0.32
53.596	H	17.6	27.3	37.5 × 37.5	0.33
54.4	H	17.6	27.3	37.5 × 37.5	0.33
55.5	H	17.6	27.3	37.5 × 37.5	0.34
57.29	RC	17.6	27.3	37.5 × 37.5	0.41
59.4	RC	17.6	27.3	37.5 × 37.5	0.40
63.283248 ± 0.285271	RC	17.6	27.3	75 × 75	2.7
60.792668 ± 0.357892	RC	17.6	27.3	75 × 75	2.7
60.792668 ± −0.357892 ± 0.002	RC	17.6	27.3	75 × 75	1.9
60.792668 ± 0.357892 ± 0.005	RC	17.6	27.3	75 × 75	1.3
60.792668 ± 0.357892 ± 0.016	RC	17.6	27.3	75 × 75	0.8
60.792668 ± 0.357892 ± 0.050	RC	17.6	27.3	75 × 75	0.9
91.665	H, V	14	13	13 × 16	0.19
150	H	14	13	13 × 16	0.53
183.311 ± 1	H	14	13	13 × 16	0.38
183.311 ± 3	H	14	13	13 × 16	0.39
183.311 ± 6.6	H	14	13	13 × 16	0.56

ICI-like

Task 1. (SH) Antartic ice shelf targets

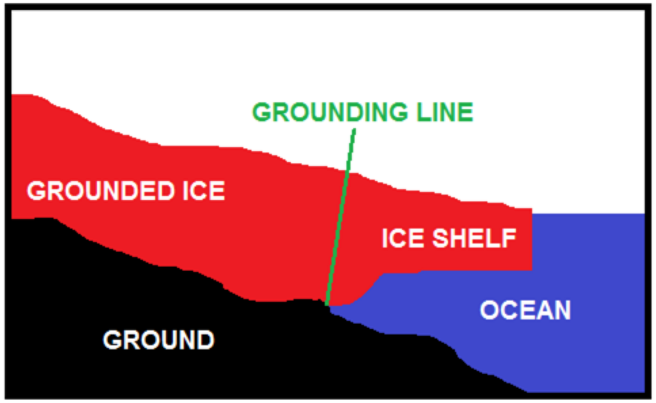

Problems:

- **ice shelfs are in movement …** but, their average speed is from 300-1000 meters/year
- the grounding line dataset is useless …!?

F17 SSMIS at 183±7 GHz H

Ross Ice Shelf

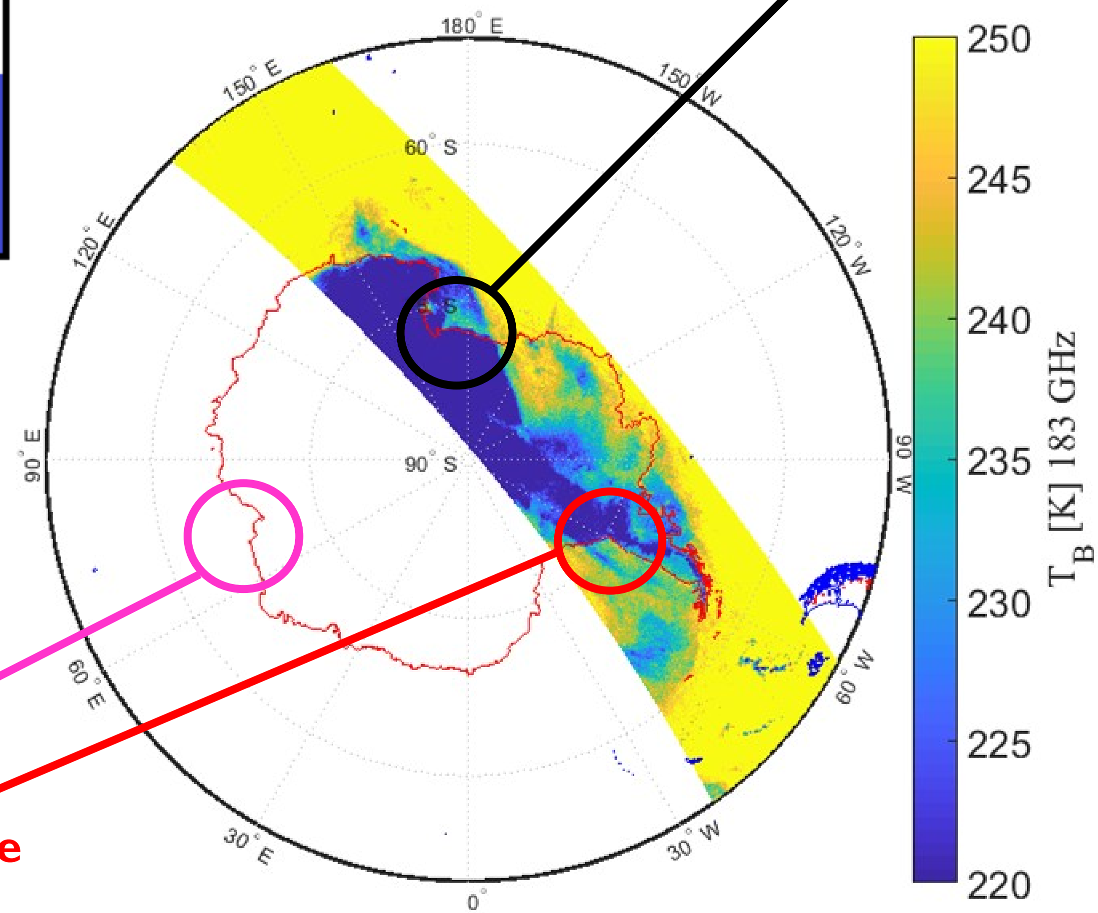

Amery Ice Shelf

Filchner-Ronne Ice Shelf

Task 1. (SH) Ice shelves - Exploiting Sentinel 1 SAR

C-band SAR

- Centre frequency: 5.405 GHz
- Polarisation:
  VV+VH, HH+HV, HH, VV
- Incidence angle: 20° - 45°
- Radiometric accuracy: 1 dB

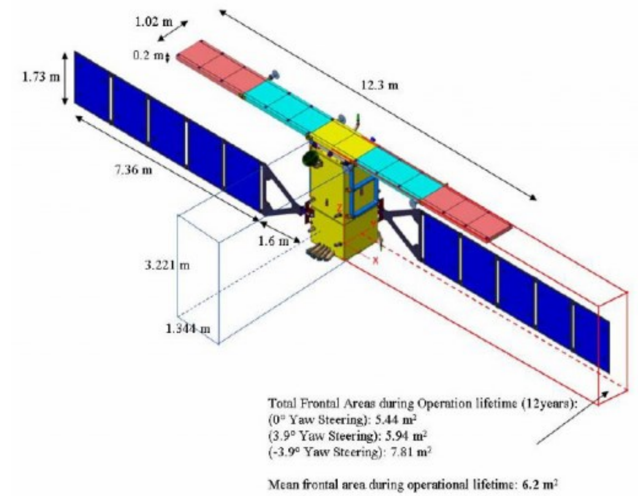

Modes, Swatch Widths and Resolutions

- Strip Map Mode:
  80 km swath, 5 x 5 m spatial resolution
- Interferometric Wide Swath:
  250 km swath, 5 x 20 m spatial resolution
- Extra-Wide Swath Mode:
  400 km swath, 20 x 40 m spatial resolution
- Wave-Mode:
  20 x 20 km, 5 x 5 m spatial resolution.

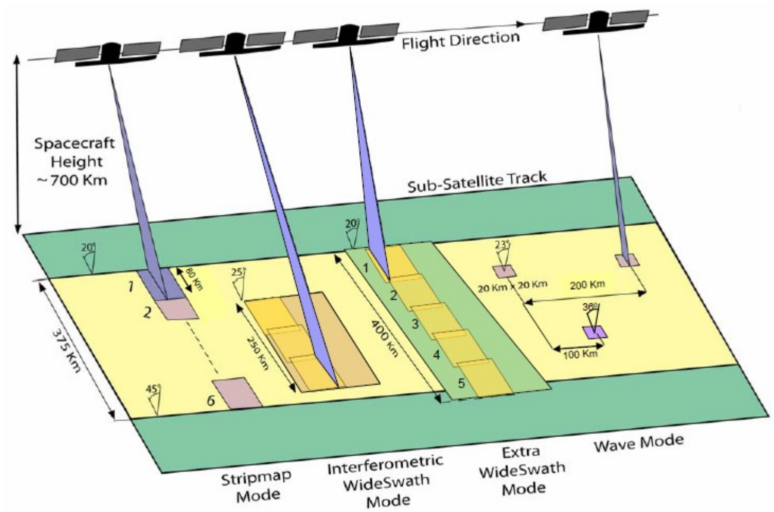

Task 1. (SH) Ice shelves - Using S1 SAR reference

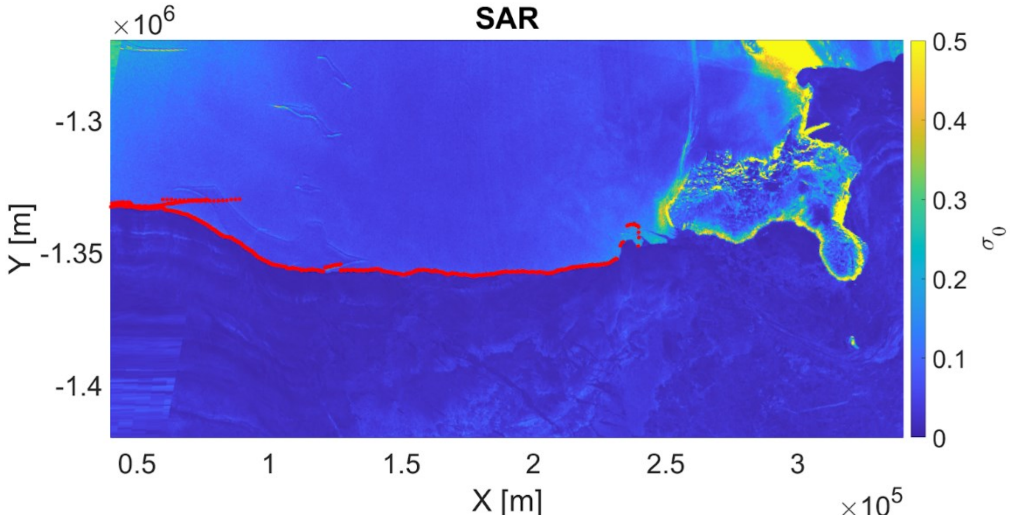

Ross ice shelf
Example of Sentinel-1 SAR image (EW mode) backscattering coefficient, to extract a contour used as reference within TCM

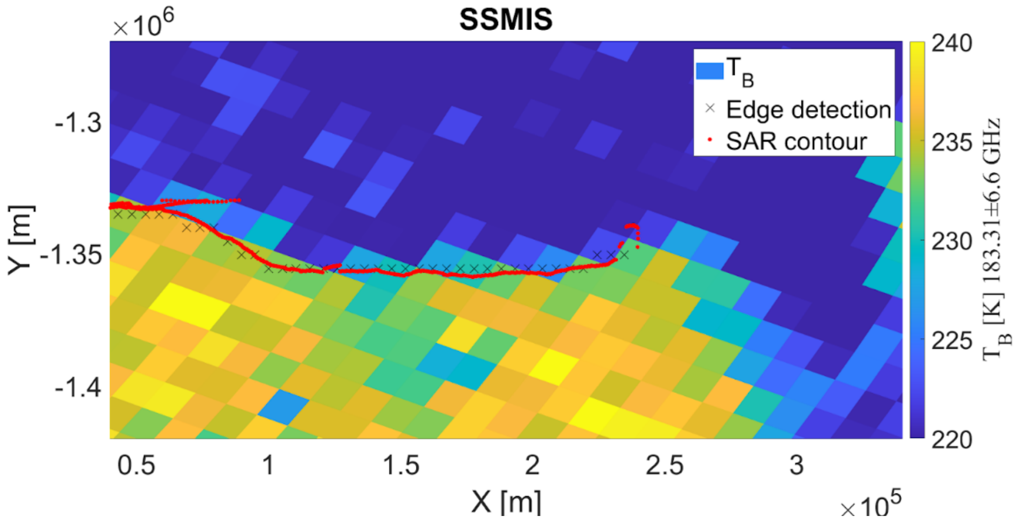

Ross ice shelf
SSMIS brightness temperature over the Ross ice shelf from SSMIS F17 at 183±7 GHz (horizontally polarized)

The red line represents the GSHHG shoreline database and black markers are provided by edge detection from SSMIS radiometric image

Task 1. (SH) High-altitude lakes – Titicaca Lake

Titicaca lake

Titicaca lake is a large, deep lake in the Andes on the border of Bolivia and Peru. It has a surface of about 8372 km^2 and an elevation o f 3812 m

Reference source: GSHHG (Global Self-consistent Hierarchical High-resolution Geography, Wessel-Smith , JGR SE 1996) shoreline database

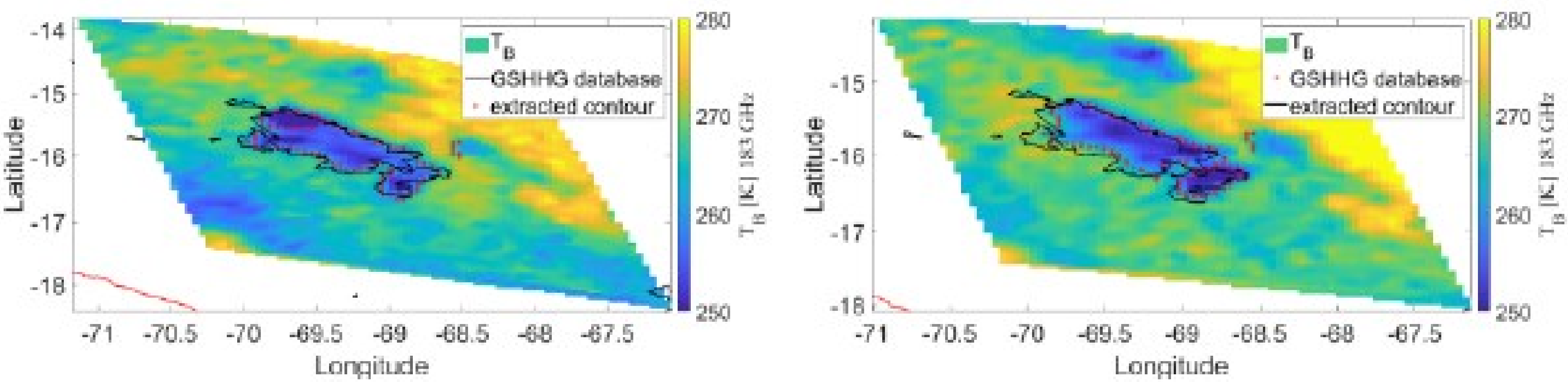

EXAMPLE. Brightness temperature image at 183±6.6 GHz H over Titicaca lake with SSMIS F17 on 2016/05/31 (left) and 2016/07/31 (right). The red markers represent the GSHHG shoreline database and black markers are provided by Canny edge detection from radiometric images..

Task 1. Parallax error correction for high targets

- The satellite coordinates are projected on WGS84 (ellipsoid)
- If a target is above the sea level

It is necessary to correct the coordinates introducing Digital Elevation Model (DEM):

- ACE2
- SRTM30
- SRTM3
- GTOPO 30

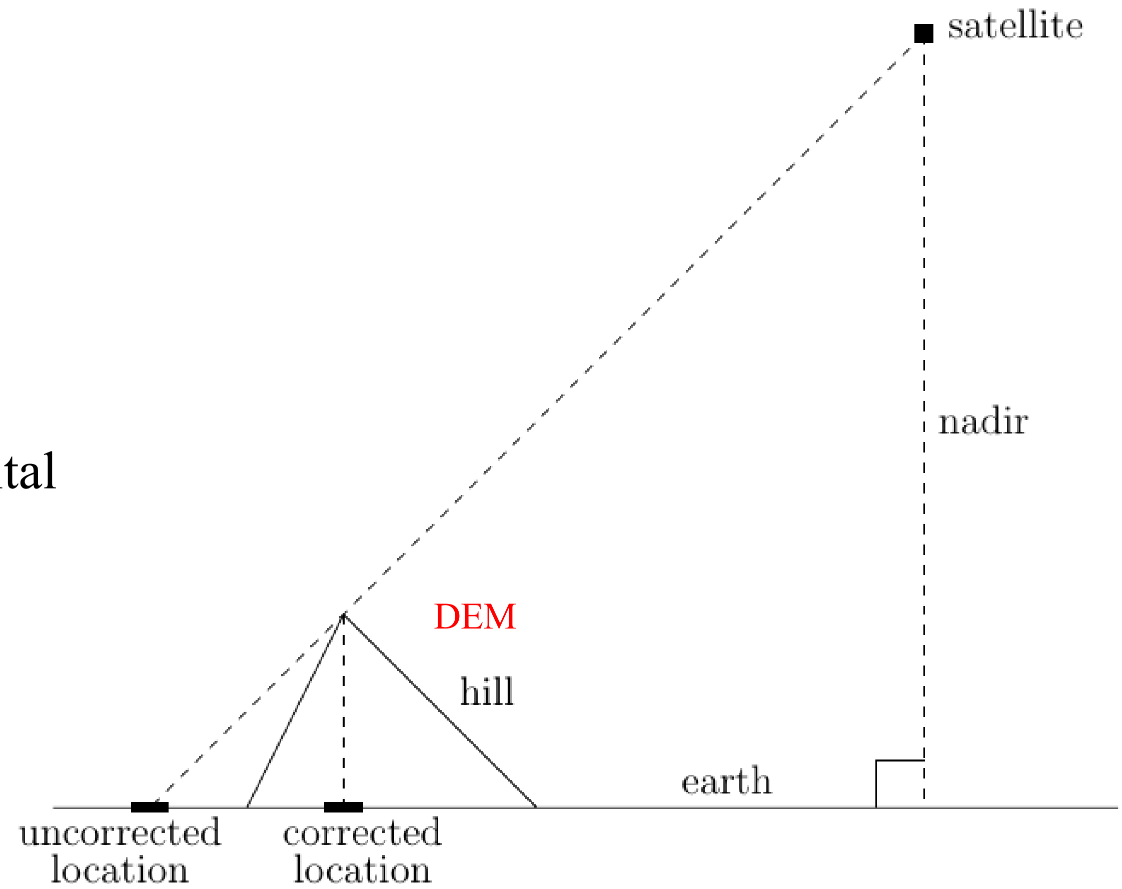

Task 1. Parallax correction with DEM

For each single grid point

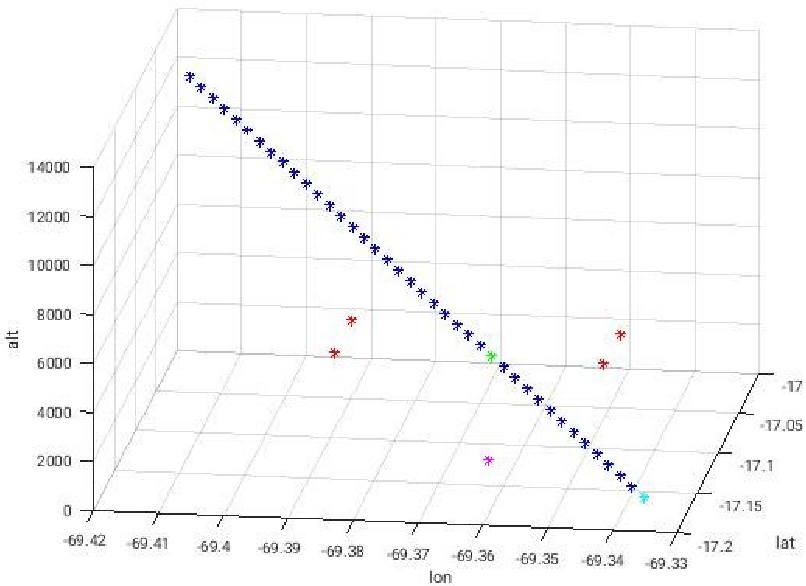

LEGEND

- Line of sight
- 4 nearest points of DEM
- First point of the line of sight that has an altitude lower than DEM
- Intersection between line of sight and earth ellipoid (WGS84)
- Corrected coordinates of surface

Example: Titicaca lake

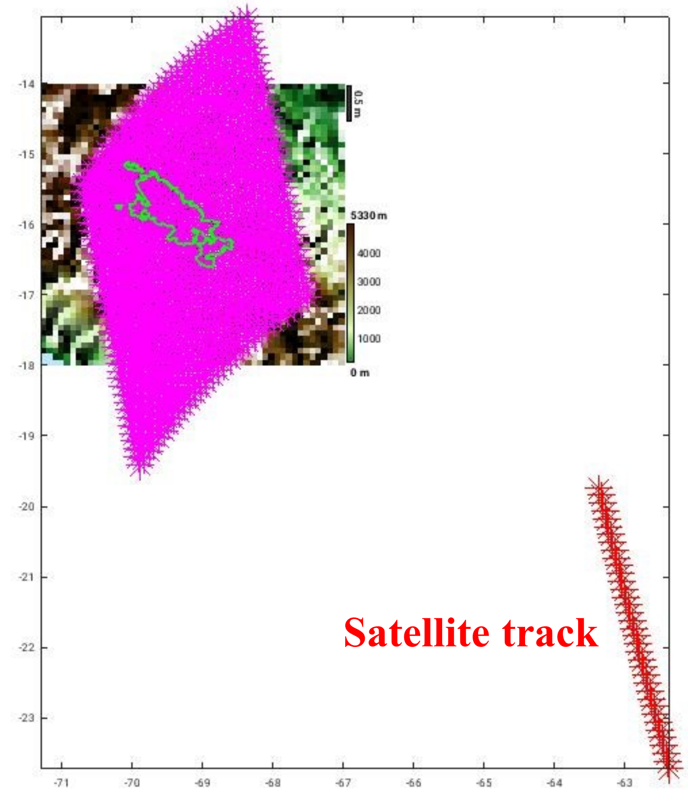

Note: parallax correction must be carried out for the whole image

Task 1. (SH) Mountain chain slopes - Andes

Andean mountains

Andean mountains are the longest continental mountain range in the world, forming a continuous highland a long the western edge of South America.

Reference source: GTOPO30 digital elevation model (Gesh et al., Eos Trans. 1999)

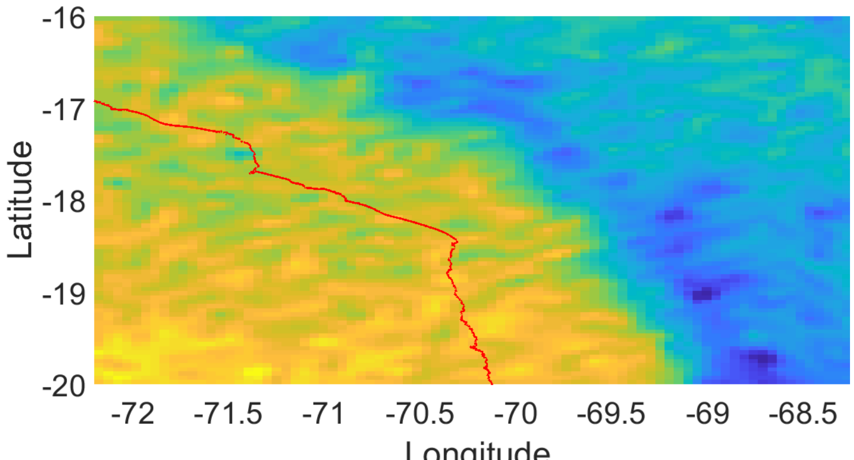

Brightness temperature over Andean mountains from SSMIS F17 at 183±6.6 GHz (H polarized) on 2016/07/14

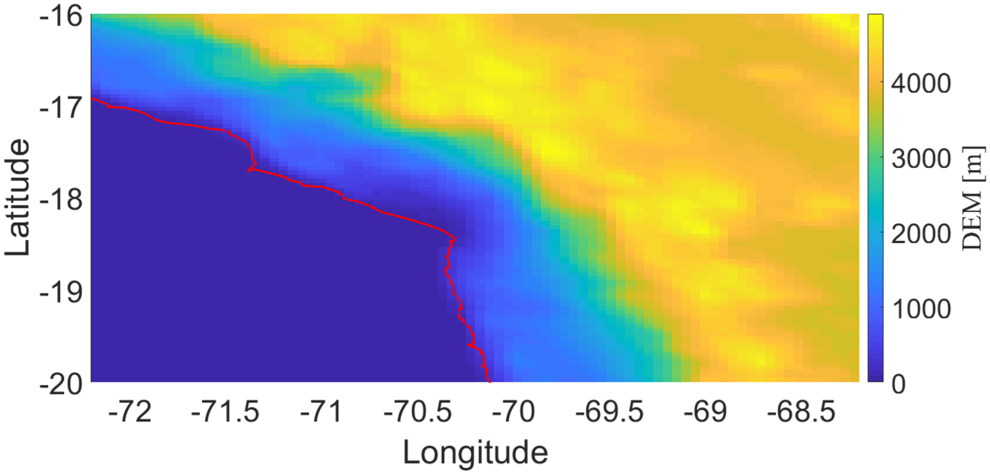

Digital elevation model (DEM), over Andean Mountains.

Task 1. (NH) High-altitude lakes – Qinghai Lake

Qinghai lake

Qinghai Lake (or Ch'inghai Lake) is the **largest lake in Chin**a. Located in an endorheic basin in Qinghai Province, to which it gave its name, Qinghai Lake is classified as an alkaline salt lake

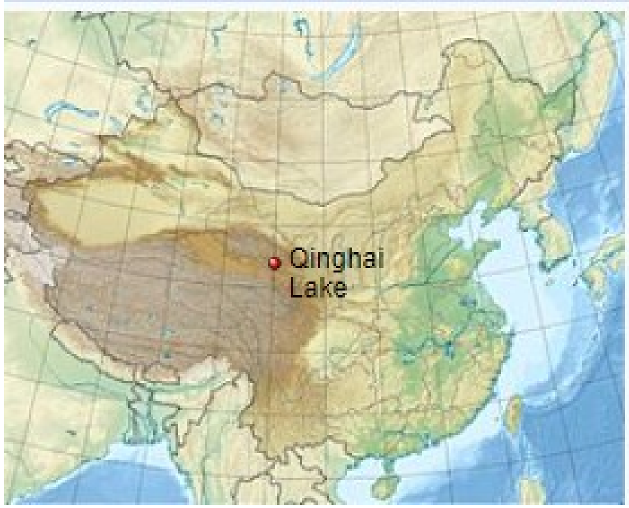

Reference source: GSHHG (Global Self-consistent Hierarchical High-resolution Geography, 1996) shoreline database

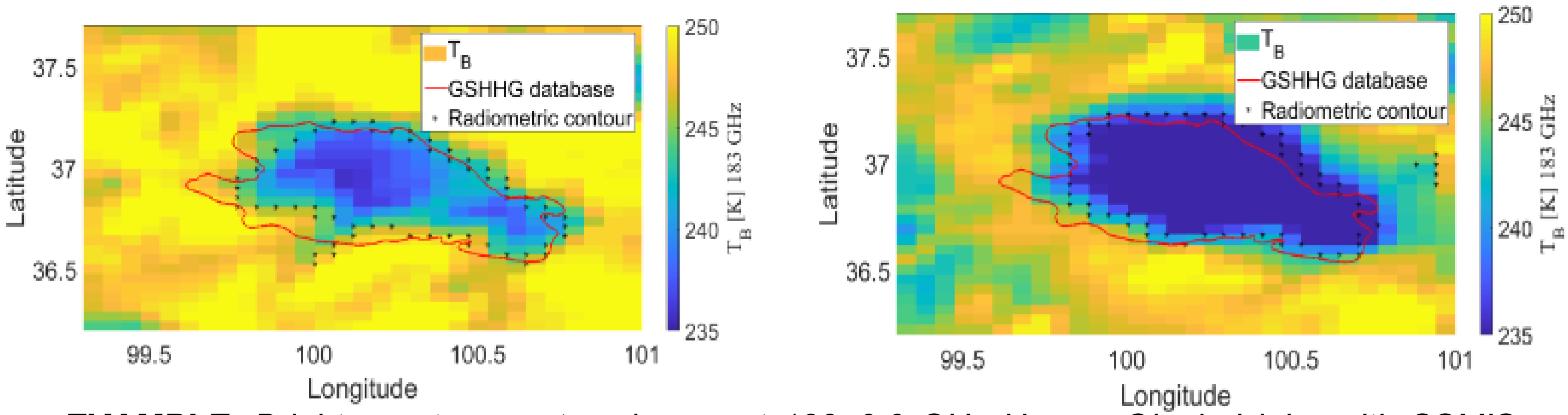

EXAMPLE. *Brightness temperature image at 183±6.6 GHz H over Qinghai lake with SSMIS F17 on 2016/12/01 (left) and 2016/12/02 (right). The red line represents the GSHHG shoreline database and black markers are provided by Canny edge detection from radiometric image.*

Task 1. (NH) Mountain chain slopes - Karakorum

Karakorum mountains

Large mountain range spanning the borders between Pakistan, India and China with the northwest extremity of the range extending to Afghanistan and Tajikistan

Reference source: GTOPO30 digital elevation model (Gesh et al., Eos Trans. 1999)

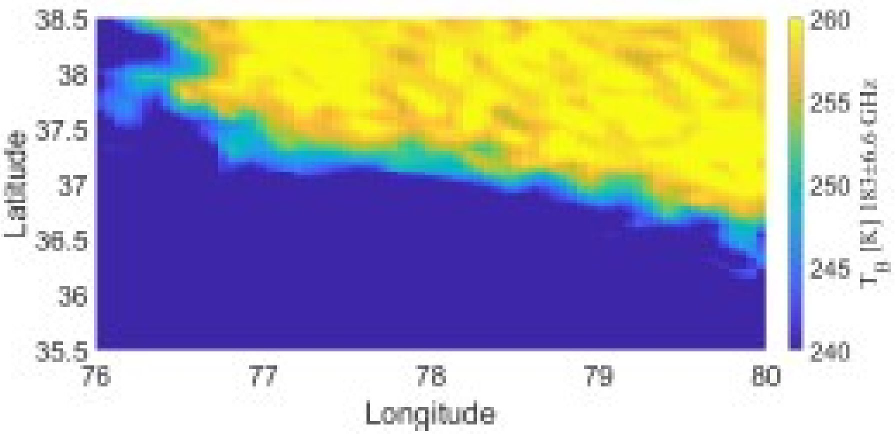

Brightness temperature over Andean mountains from SSMIS F17 at 183±6.6 GHz (H polarized) on 2016/10/19

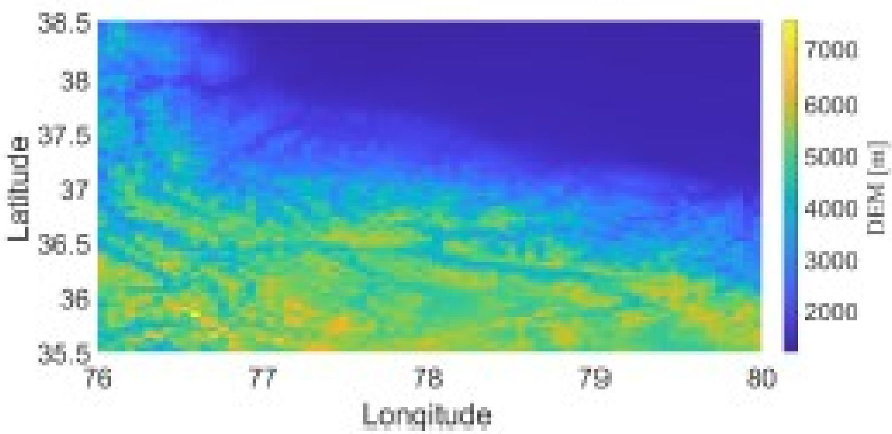

Digital elevation model (DEM), over Andean Mountains.

Task 1. (NH) High-latitude bay - Hudson

Hudson bay

Large body of saltwater in northeastern Canada with a surface area of 1,230,000 km^2.

Reference source: GSHHG (Global Self-consistent Hierarchical High-resolution Geography, 1996) shoreline database

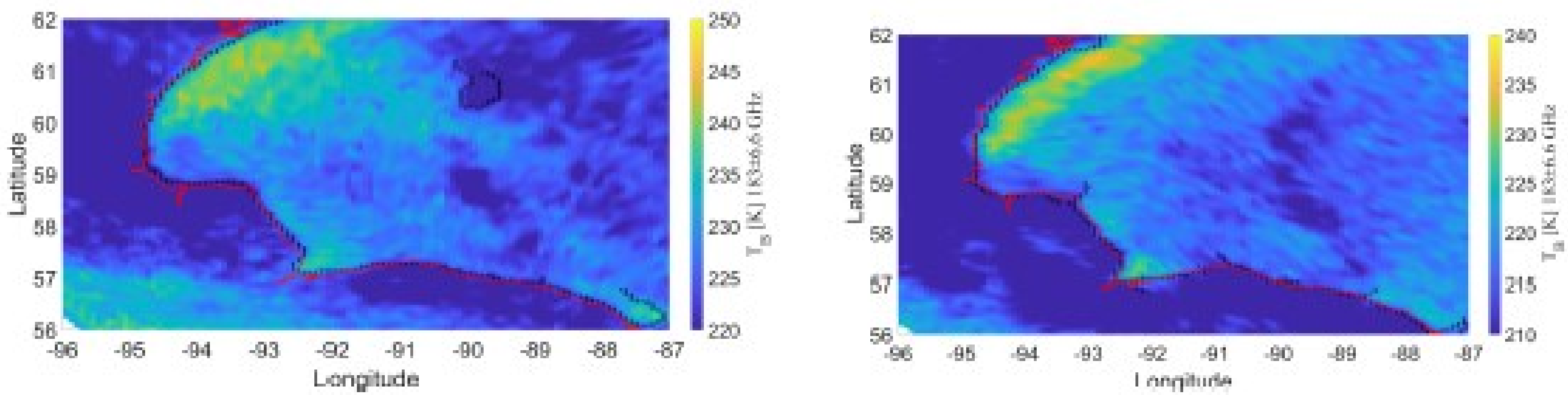

EXAMPLE. *Brightness temperature image at 183±6.6 GHz H over the Hudson bay with SSMIS F17 on 2016/01/27 (left) and 2016/02/11 (right). The red line represents the GSHHG shoreline database and black markers are provided by Canny edge detection from radiometric image.*

Task 1. (NH) High-latitude strit - Nares

Nares Strait

Nares Strait, that is a waterway between Ellesmere Island and Greenland that connects the northern part of Baffin Bay with the Lincoln Sea

Reference sources: GSHHG (Global Self-consistent Hierarchical High-resolution Geography, 1996) shoreline database and Setninel-1 SAR contour detection

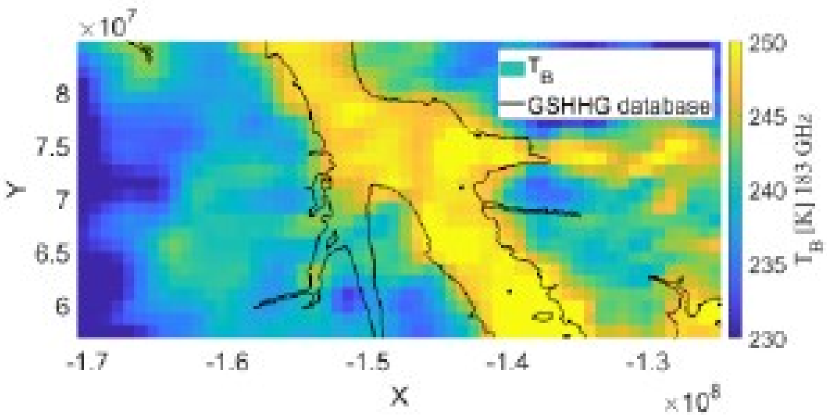

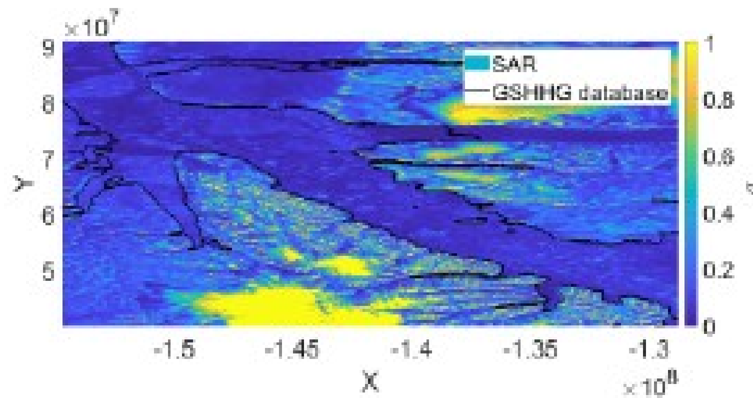

EXAMPLE. *Brightness temperature image at 183±6.6 GHz H over Nares Strait from SSMIS F17 on 2016/11/02 (left), the black line is provided by GSHHG shoreline database. SENTINEL 1 IW-GRD on 2017/01/12 (right)*

Outline

- **GAMES project**
- **GAMES rationale and objectives**
- **Task 1. Landmark target methodology**
  - Searching for ICI surface landmark targets
  - Results of ICI geolocation assessment
- **Task 2. Atmospheric target approach**
  - ICI absolute geolocation using DCC and WVM
  - ICI relative geolocation using BG approach
- **Task 3. Geolocation algorithm implementation**
- **Conclusion**

Task I. Geolocation assessment targets

9 selected landmark targets: 4 in NH, 5 in SH

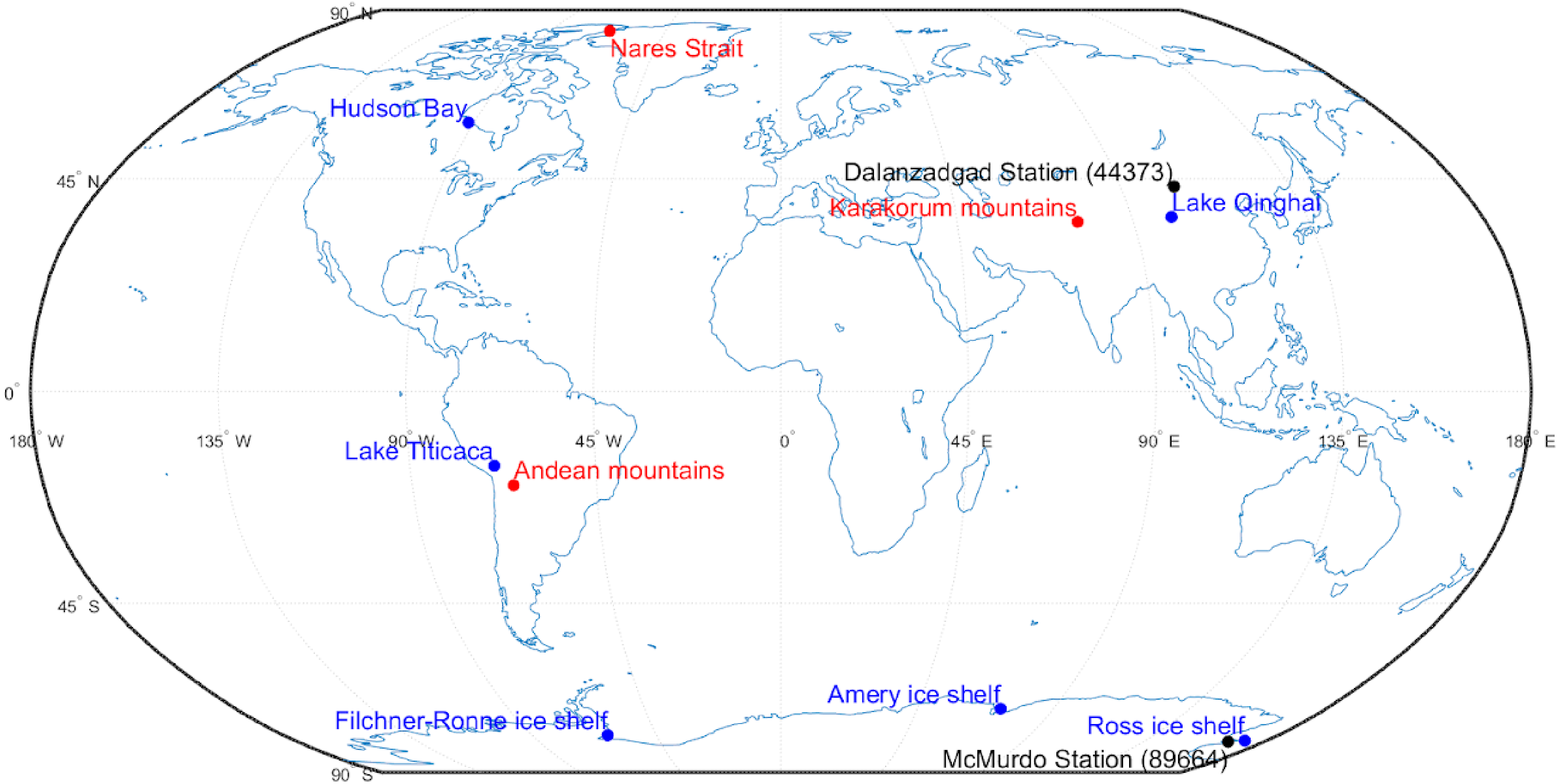

Task 1. Automatic clear-air target image selection

Along the entire year we have many swaths covering different targets

e.g.: - Ross ice shelf more than 2000 samples
- Qinghai lake more than 600 samples

Each satellite swath can be used if:

- No presence of clouds within the region of interest (ROI)
- High enough BT contrast to extract the contour

GOAL: apply a fuzzy-logic approach to discriminate cloudy/clear regions

Theory of fuzzy sets (L. Zadeh, 1965-68)

1. Fuzzification step: memership function and inference function
2. Defuzzification step: output value and decision

Task 1. Clear-air target selection: defuzzification step

Example: Qinghai Lake

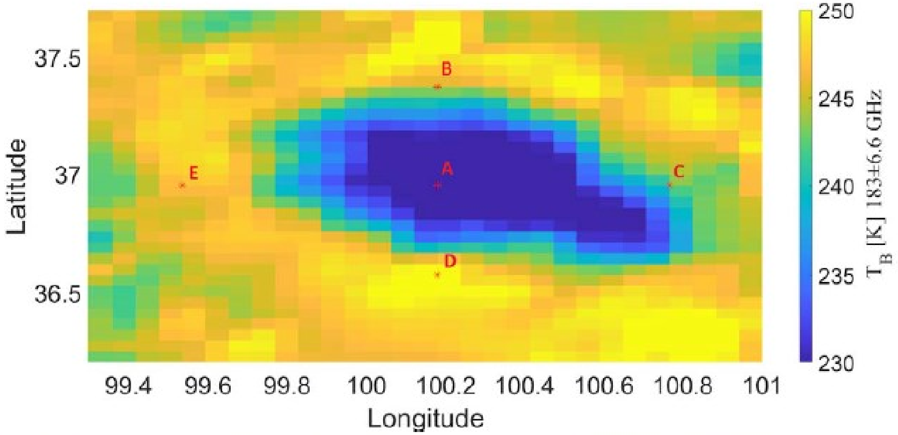

Figure A.1: Brightness temperature (BT) image at 183±6.6 GHz H over Qinghai lake from SSMIS F17 on 2016/12/01. Five points are those used to calculate the BT contrast along vertical and horizontal directions

$$I(x) = M_1(x)\, M_2(x)$$

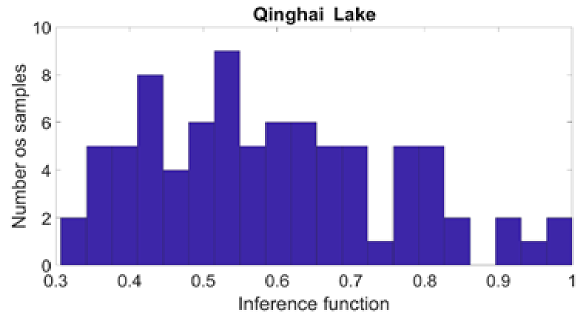

Image can be used if $I(x) \geq I_{threshold}$

$$M_2 = \begin{cases} linear & \Delta T_B \leq \Delta T_{B\ threshold} \\ 1 & \Delta T_B > \Delta T_{B\ threshold} \end{cases}$$

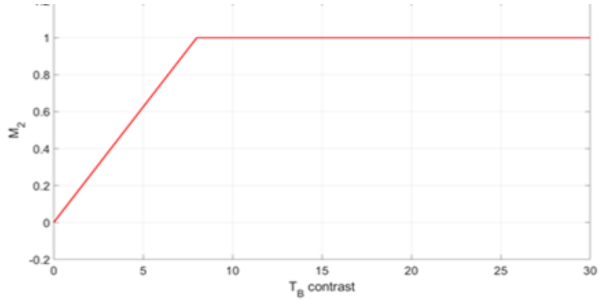

$$M_1 = \begin{cases} linear & Error \leq Error_{threshold} \\ 0 & Error > Error_{threshold} \end{cases}$$

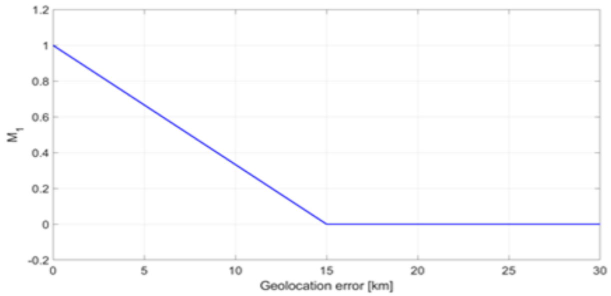

Task 1. Target contour matching (TCM) algorithm

CONTOUR EXTRACTION - EDGE DETECTION APPROACHES

- the Canny approach [9] to extract a line. This method consists of the following main steps:
    1. Convolution with Gaussian filter coefficient
    2. Convolution with Canny filter for horizontal and vertical orientation
    3. Calculating directions using atan2
    4. Thresholding

All targets except mountain chain slopes

- the Sobel filter [13] to obtain a gradient map. This method consists of the following main steps:
    1. Convolution with two matrices to compute the derivative along x and y
    2. Computing the gradient magnitude

Mountain chain slopes

Target contour matching (TCM) – Landmark

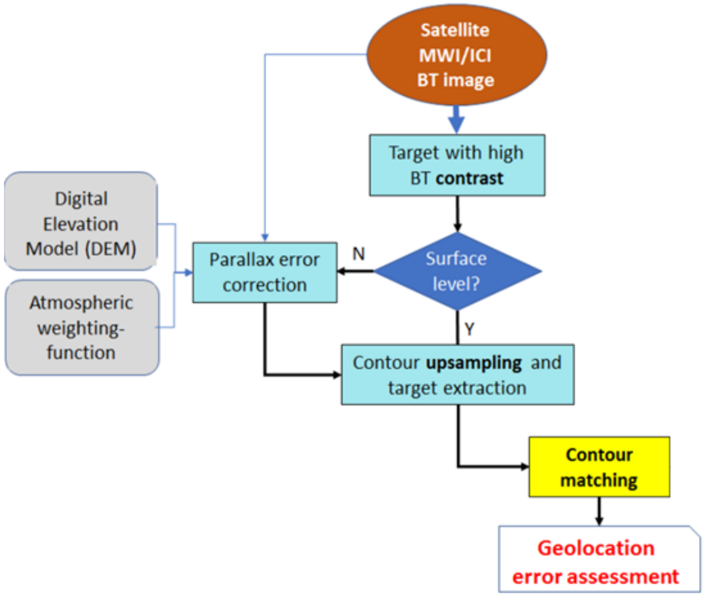

Fast normalized cross-correlation (FNC)
(Canny, TPAAI, 1986)

$$\gamma(u,v) = \frac{\sum_{x,y}\left[f(x,y)-\bar{f}_{u,v}\right]\left[t(x-u,y-v)-\bar{t}\right]}{\left\{\sum_{x,y}\left[f(x,y)-\bar{f}_{u,v}\right]^2 \sum_{x,y}\left[t(x-u,y-v)-\bar{t}\right]^2\right\}^{0.5}}$$

Registration in the frequency domain (RFD)
(Guizar-Sicairos et al., OL, , 1986)

Task I. Geolocation assessment – Result table

Database

- SSMIS TB data
- Channel *183±6.6 GHz H*
- Year 2016
- (Year 2017)
- 9 landmark targets

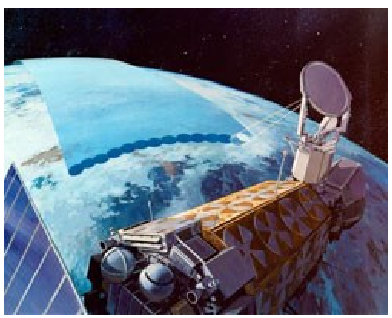

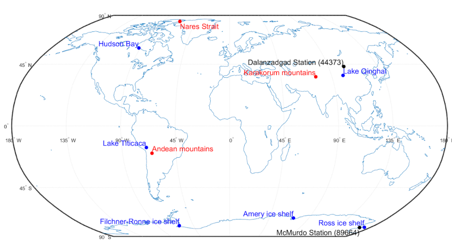

Target	Geolocation error mean value [km]	Geolocation error standard deviation [km]	Cloud-masked yearly sample number (percentage)	Notes
Northern hemisphere (NH)				
Qinghai lake	5.10	2.03	129 (20.6%)	All shift directions are sampled due to the close contour.
Karakorum mountains	4.47	1.86	302 (42.6%)	DEM resolution may impact the results. Useful oblique pattern.
Hudson Bay	5.28	2.56	135 (49.0%)	All shift directions are sampled due to the U contour.
Nares strait	4.55	1.65	587 (27.5%)	Slightly scattered contour with oblique pattern.
NH average value	*4.9 km*	*2.0 km*		
Southern hemisphere (SH)				
Ross ice shelf	5.30	2.18	725 (31.1%)	Sharp high-resolution contour, but mainly horizontal pattern.
Filchner-Ronne ice shelf	4.31	1.89	541 (22.9%)	Sharp high-resolution contour with a V contour
Amery ice shelf	5.32	2.27	242 (19.5 %)	Sharp high-resolution contour with a nearly-vertical contour
Titicaca lake	4.80	2.50	52 (9.8%)	All shift directions are sampled due to the close contour.
Andean mountains	3.70	1.95	177 (19.3%)	DEM resolution may impact the results. Useful oblique pattern.
SH average value	*4.7 km*	*2.2 km*		

Task I. Geolocation assessment – Result bars

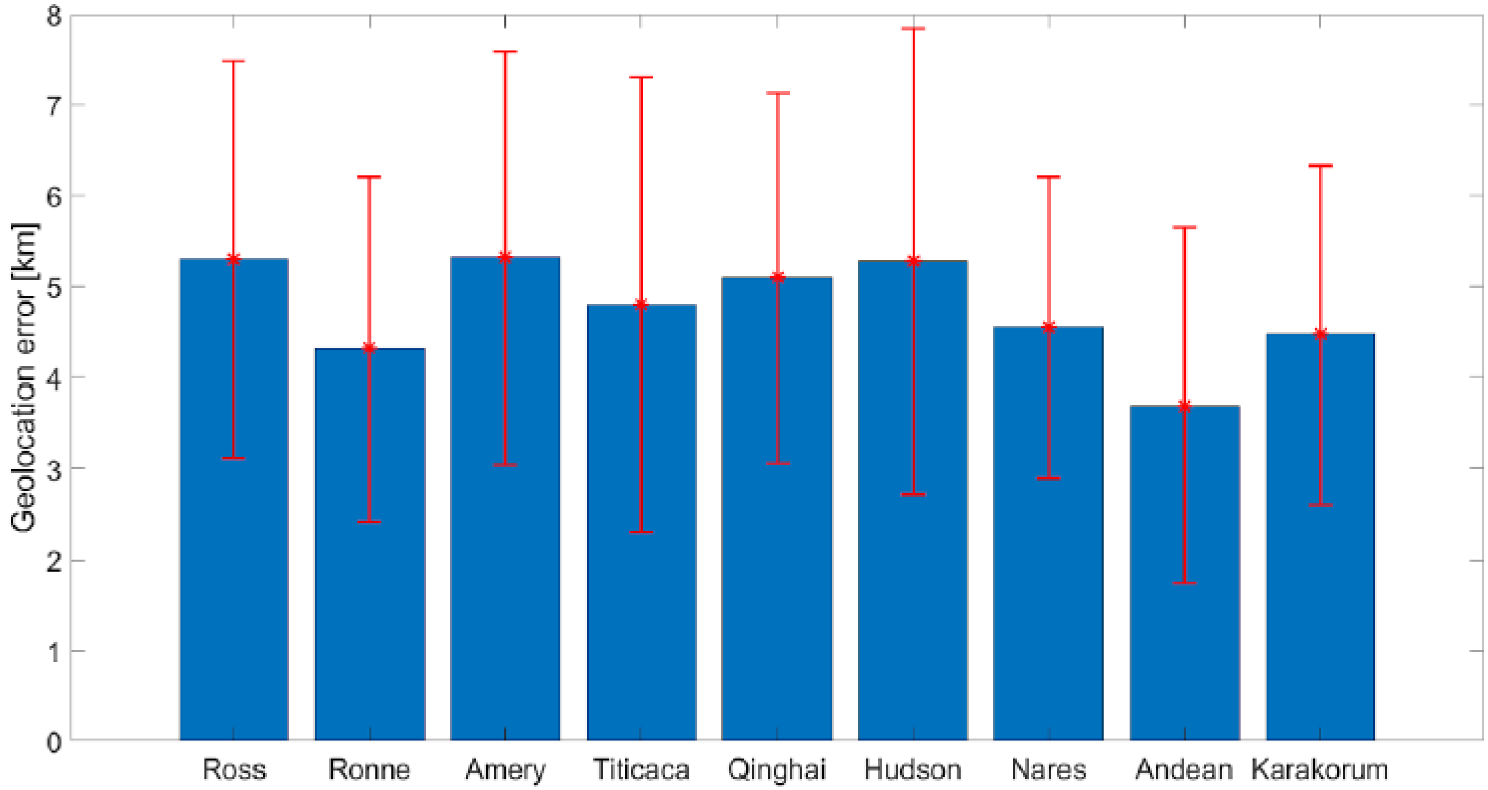

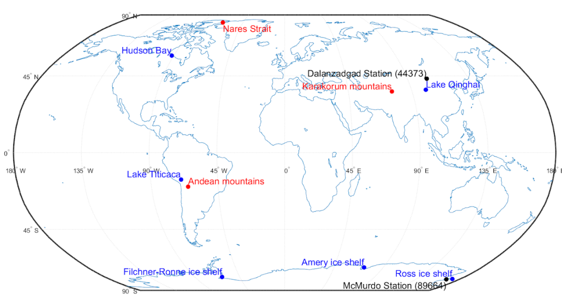

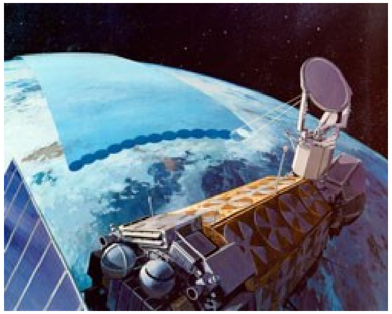

Database

- SSMIS TB data
- *Ch.: 183±6.6 GHz H*
- Year 2016
- Year 2017
- 9 landmark targets

Task I. Geolocation assessment - Sensitivity

Sensitivity parameter	Result standard deviation [km]
Interpolation-grid spatial resolution	0.62
Spatial interpolation method	0.01
Cross-correlation technique	0.04

$$\Delta = \sqrt{(0.62^2+0.01^2+0.04^2)} \sim 0.62 \text{ km}$$

The most important parameter in the geolocation assessment methodology is the spatial resolution of the interpolation grid (set to 5-km nominal value)

Impact of FL cloud masking inference thresholds

$I = inference\ function$

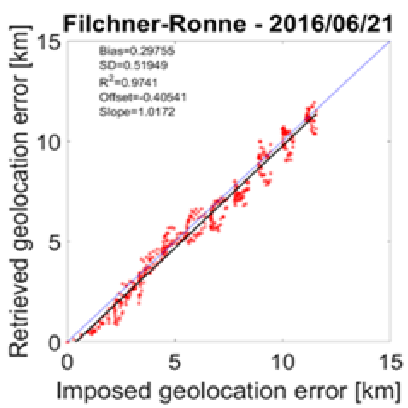

$I = 0.86$

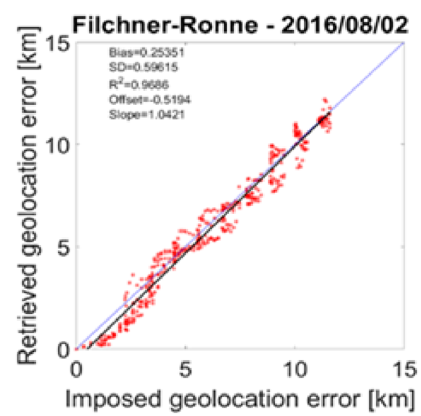

$I = 0.96$

Task I. Geolocation assessment – Detectability

Landmark target	Contour reference source	Detectability/day
	Northern hemisphere	
Qinghai lake	GSHHG	1
Karakorum mountains	DEM	1
Hudson Bay	GSHHG	1
Nares Strait	SAR	4-6
	Southern hemisphere	
Ross Antarctic ice shelf	SAR	4-6
Filchner-Ronne Antarctic ice shelf	SAR	4-6
Amery Antarctic ice shelf	SAR	3-5
Titicaca lake	GSHHG	1
Andean mountains	DEM	1

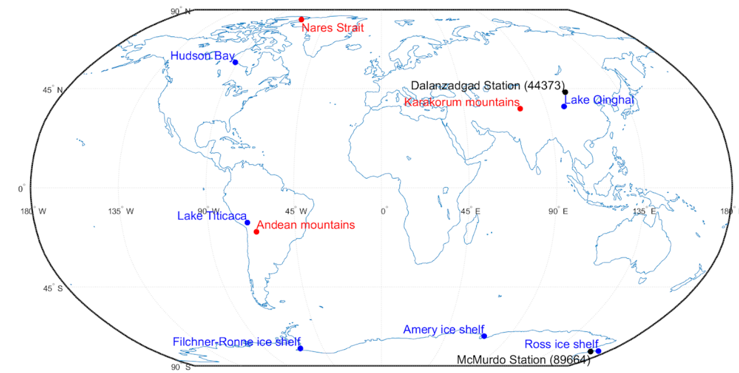

Target	$\delta_{th} = 1\%$		$\delta_{th} = 2\%$	
	n_{opt}	n_{optdd}	n_{opt}	n_{optdd}
Qinghai lake	82	82	54	54
Karakorum mountains	31	31	31	31
Hudson Bay	61	61	60	60
Nares strait	518	130	446	112
Ross ice shelf	286	72	166	42
Filchner-Ronne ice shelf	245	62	80	20
Amery ice shelf	142	36	127	31
Titicaca lake	-	-	16	16

NOTE

n_{opt}: optimal number of target overpasses to stabilize both mean and standard deviation of the error geolocation

n_{optdd}: optimal number of days to stabilize both mean and standard deviation of the error geolocation

Conclusions on Task 1 and future work

- Using the **183±6.6 GHz H** from SSMIS F17 using a whole year dataset (2016) we obtain an overall estimate of **geolocation assessment error** with a:
  - average value of about *4.8 km*
  - standard deviation of about *2.1 km*

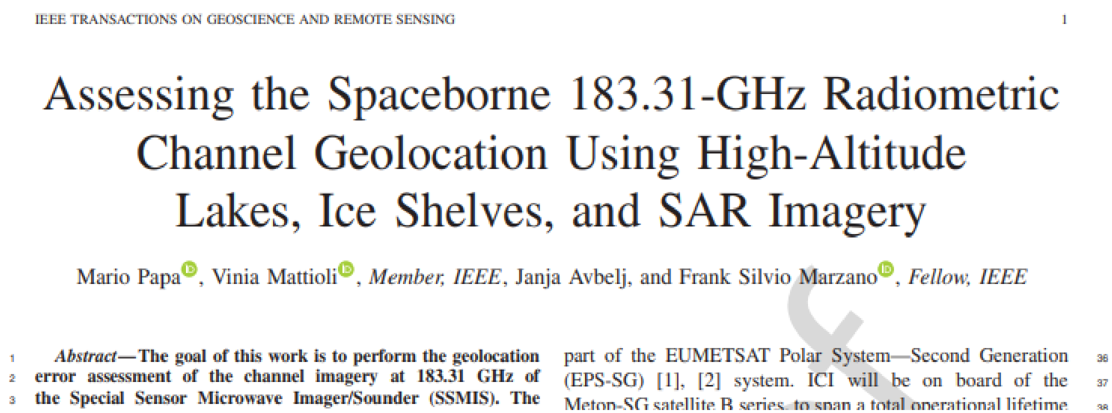

IEEE TRANSACTIONS ON GEOSCIENCE AND REMOTE SENSING 1

Assessing the Spaceborne 183.31-GHz Radiometric Channel Geolocation Using High-Altitude Lakes, Ice Shelves, and SAR Imagery

Mario Papa, Vinia Mattioli, *Member, IEEE*, Janja Avbelj, and Frank Silvio Marzano, *Fellow, IEEE*

***Abstract*—The goal of this work is to perform the geolocation error assessment of the channel imagery at 183.31 GHz of the Special Sensor Microwave Imager/Sounder (SSMIS). The**

part of the EUMETSAT Polar System—Second Generation (EPS-SG) [1], [2] system. ICI will be on board of the Metop-SG satellite B series, to span a total operational lifetime

The standard atmosphere is on average **more transparent at 243 GHz than 183 GHz**, so that further work should focus on the investigation of ICI-4 (243±2.5 GHz H)

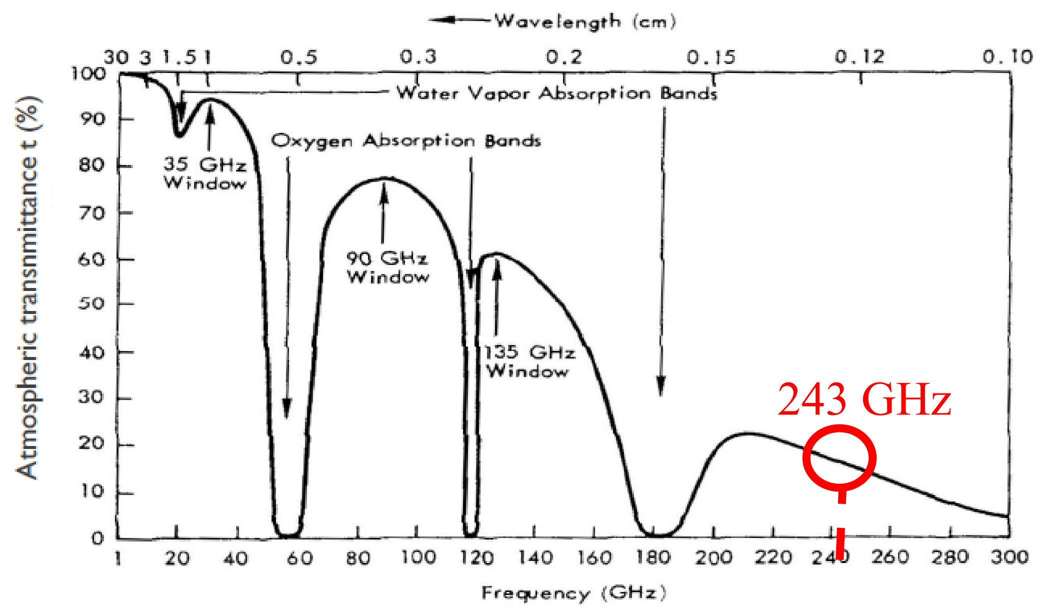

ICI channels simulation - 1D radiative transfer model

ERA 5 (ECMWF Re-Analyses 5)

- 3D atmospheric variables to simulate the entire scene
- 31 km of spatial resolution
- 137 vertical levels

Simulating BT at ICI 243-GHz

1. Use ERA5 as input resampled at 15 km
2. Use a radiative transfer code
3. Estimate surface emissivity
4. Simulate BT at 15-km resolution

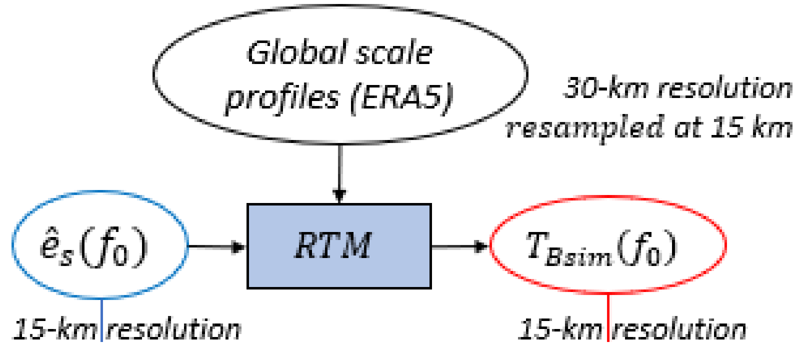

SSMIS December 1, 2016 at 11:00 UTC

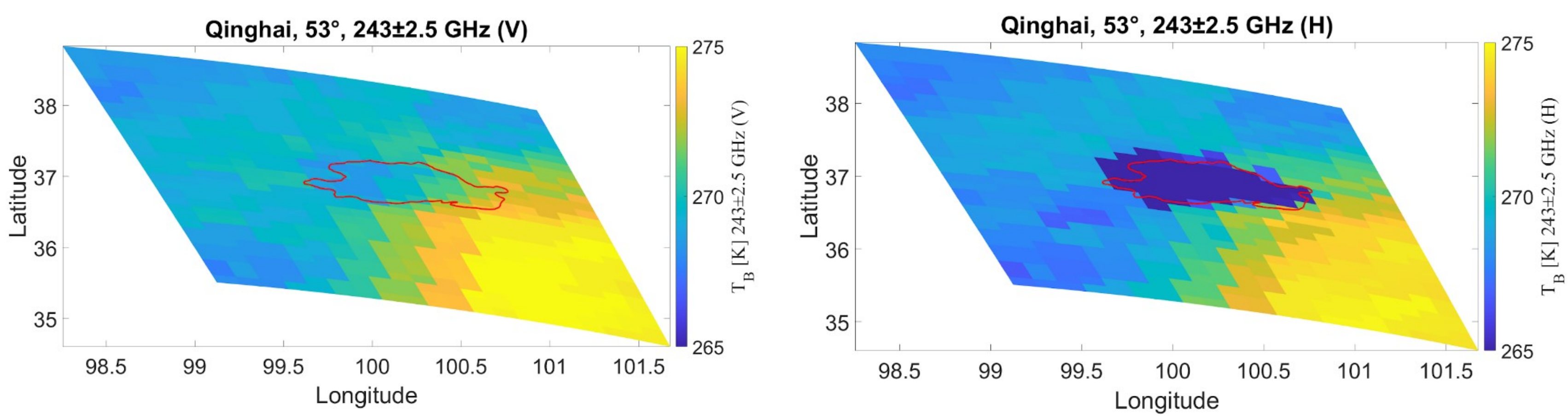

BT simulations for **ICI-4 at horizontal polarization show better BT contrast**

Surface emissivity estimator

From radiative transfer equation:

$$B_{sat} = e_s\, B_S\, t + B_{up} + B_{dw}(1-e_s)t + B_{bg}\,(1-e_s)\, t^2$$

we can estimate the surface emissivity (e_s)

$$e_s = \frac{\left(B_{sat} - B_{up} + B_{dw}\, t - B_{bg}\, t^2\right)}{B_S\, t - B_{dw}\, t - B_{bg}\, t^2}$$

- B_{sat} is the satellite brightness
- B_s is the surface brightness
- e_s is the surface emissivity
- t is the transmittance.
- B_{up} is the atmospheric upwelling,
- B_{dw} is the atmospheric downwelling and
- B_{bg} represents the background contributior

SSMIS December 1, 2016 at 11:00 UTC

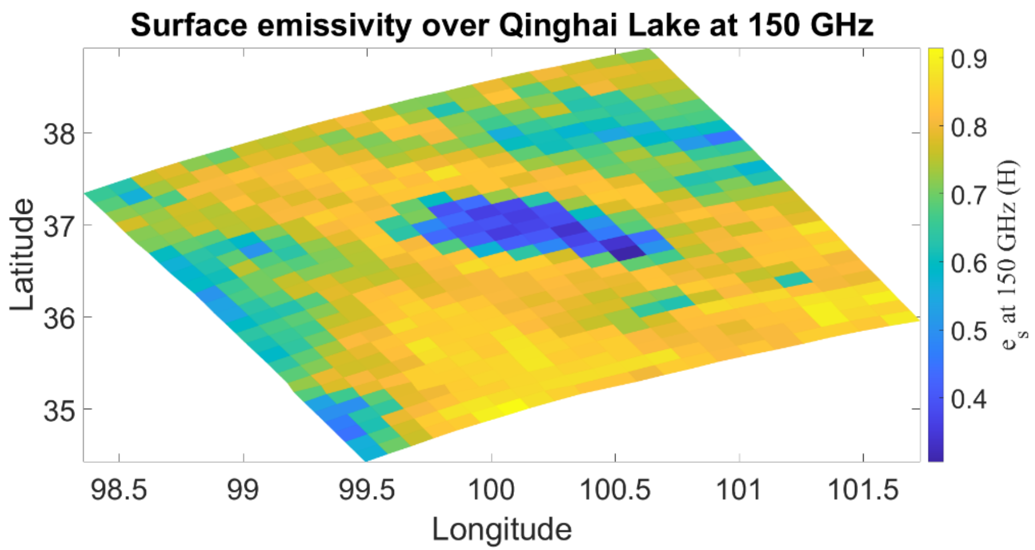

The estimated surface emissivity can show errors due to:

- low spatial resolution of surface variables provided by ERA-5
- unrealistic values of surface emissivity
- radiative transfer plane-parallel and specular surface assumptions

BAMIS (Blended ANN Microwave Imager Simulator)

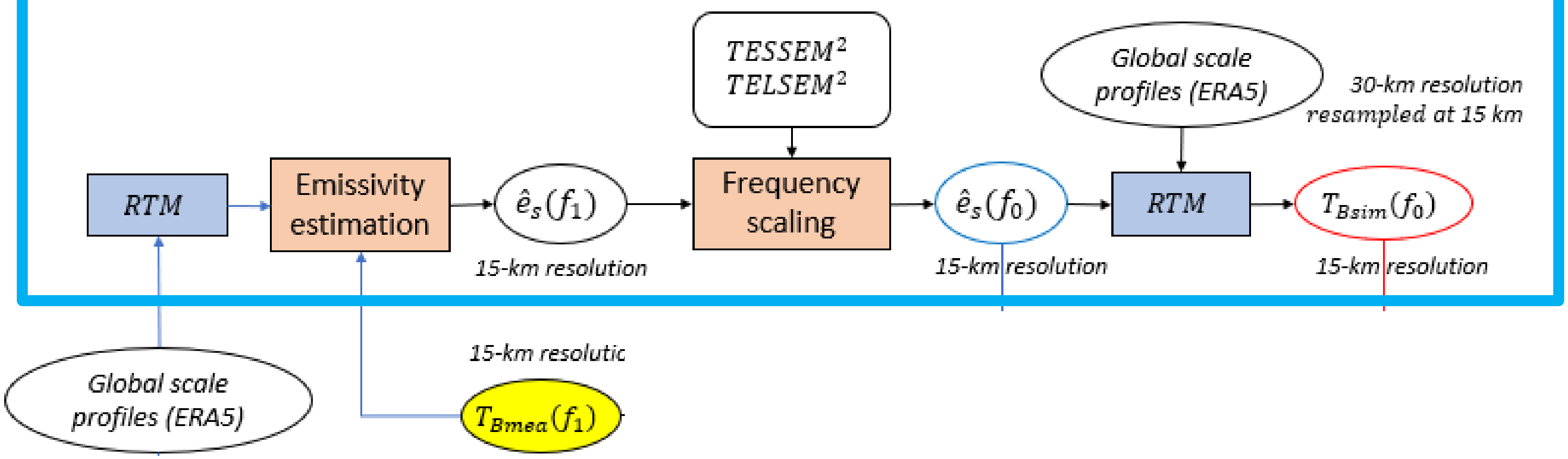

ICI simulation – ANN to reconstruct 243 GHz

Feed-forward MLP neural network (1 HL, 10 nodes)

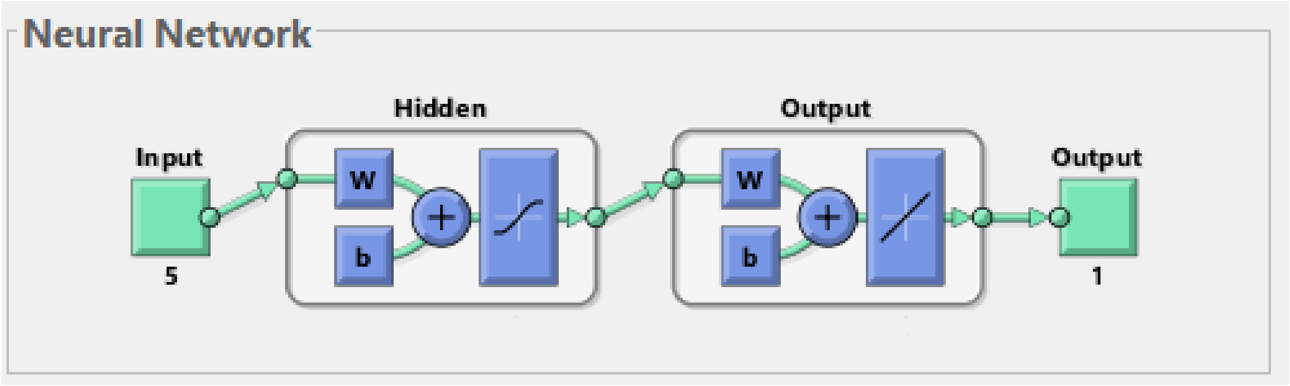

Inputs:

1. TB at 150 GHz (H)
2. TB at 183.31±6.6 GHz (H)
3. ERA5-based atmospheric transmittance at 243.2±2.5 GHz
4. Pixel latitude
5. Pixel longitude

TB at 243 GHz (H)

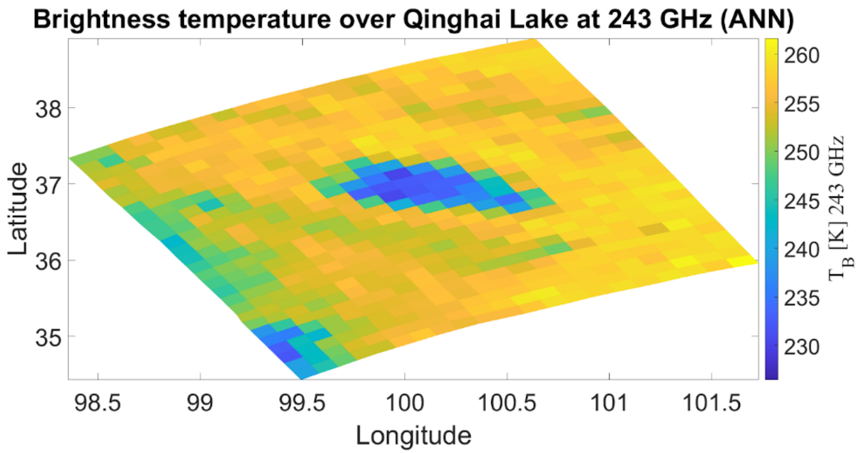

Results using BAMIS to reconstruct ICI 243 GHz

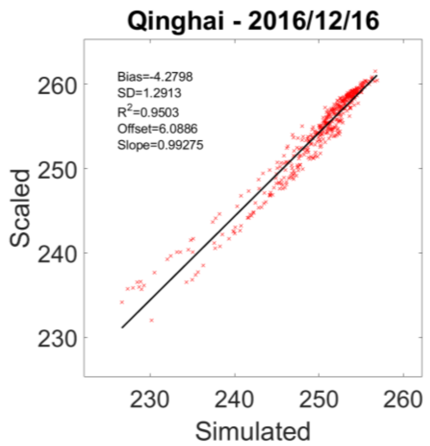

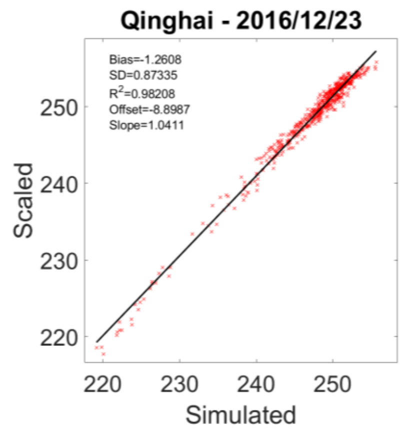

Results obtained for 2 test cases using 7 cases to train the ANN (3917 pixels)

Results for Qinghai lake from October 2016 to December 2016

Source	Geolocation accuracy average [km]	Geolocation accuracy standard deviation [km]
183.31±6.6 GHz (H) SSMIS	4.98	2.15
183.31±6.6 GHz (H) ANN	5.61	2.59
243.2±2.5 GHz (H) ANN	5.94	2.31

Outline

- **GAMES project**
- **GAMES rationale and objectives**
- **Task 1. Landmark target methodology**
  - Searching for ICI surface landmark targets
  - Results of ICI geolocation assessment
- **Task 2. Atmospheric target approach**
  - ICI absolute geolocation using DCC and WVM
  - ICI relative geolocation using BG approach
- **Task 3. Geolocation algorithm implementation**
- **Conclusion**

Block diagram of GAMES approach

Target contour matching (TCM) – Landmark and Atmospheric targets

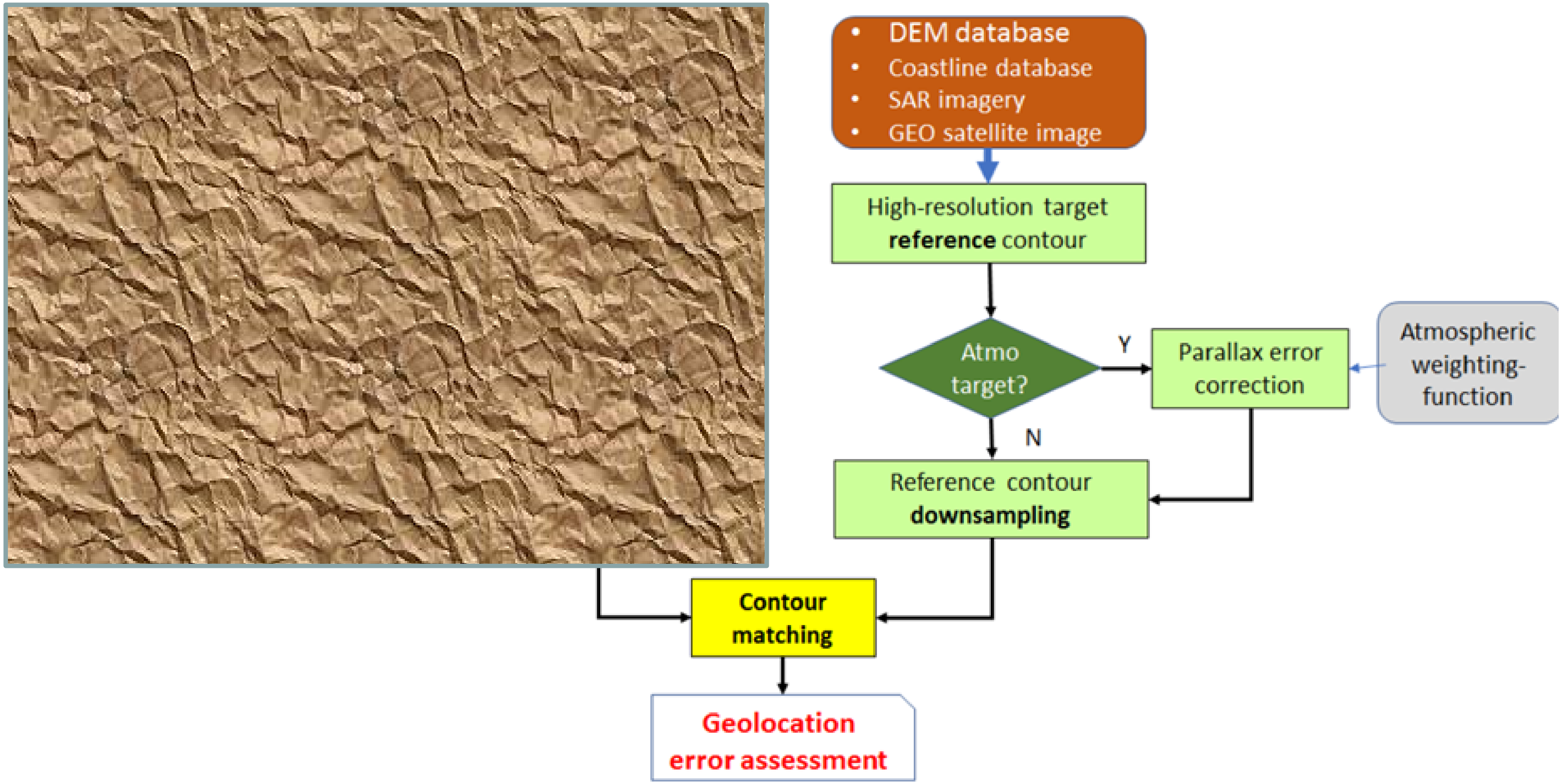

Task 2. Atmospheric targets for geolocation

- **Motivation:**
  - Geolocation is traditionally performed looking at water-land separation
  - ICI channels (f≥325 GHz) have no chance to sample the surface.
- **Goal**
  - Exploit atmospheric features for geolocating ICI channels.

Advantages: No need to have surface visibility for all channels
Likelihood to sample robust statistic during sat. overpasses

Drawbacks: Atmospheric features vary in space and time and among channels.
Use of external information for the absolute approach.
Need for an automated selection of the region of interest

- **Methodology**
  - **Absolute geolocation:**
    - Look at microwave (PMW) **183 GHz** signature of Atmo targets (i.e. Deep convective clouds and water vapor masses)
    - Combine infrared (reference IR) and MW observations to geolocate
    - Existing satellite platforms are considered
  - **Relative geolocation**
    - Look at the relative Atmo. signatures among ICI ch.s (f>183GHz) with respect to a pivot reference channel.

Task 2. Data set used for absolute geolocation

Algorithm training:

17 Case studies selected orbits and target areas with **GMI-SSMIS** and **DPR/CPR**

Algorithm preliminary assessment:

17 days (all orbits) with **SSMIS-MSG**

Algorithm extensive validation :

3 months of SSMIS-MSG observations (all orbits)

Case Study Number	Case Study Date	Target Area Latitude Longitude	GEO-VIS/IR Radiometer	LEO-MW Radiometer	Other Coincident Observations
1	23/082014	03N 30E	SEVIRI	GMI ATMS	A-Train
2	24/03/2017	04S 32E	SEVIRI	GMI ATMS	A-Train
3	17/11/2015	05N 52W	SEVIRI	GMI MHS	A-Train
4	19/03/2016	06S 29E	SEVIRI	GMI	A-Train
5	18/03/2016	11S 66E	SEVIRI	GMI ATMS	A-Train
6	06/02/2017	12S 45W	SEVIRI	GMI ATMS	A-Train
7	27/12/2015	13S 63E	SEVIRI	GMI	A-Train
8	21/07/2016	18S 49W	SEVIRI	GMI ATMS	A-Train
9	04/06/2015	22N 16E	SEVIRI	GMI ATMS	A-Train
10	24/04/2014	34S 37E	SEVIRI	GMI	A-Train
11	05/09/2013	41N 14E	SEVIRI	GMI MHS	-

Case Study Number	Case Study Date	Target Area	GEO-VIS/IR Radiometer	LEO-MW Radiometer	WV pattern Typology
1	25/10/2014	Central Europe	SEVIRI	SSMIS-MHS	Atmospheric River
2	19/02/2011	Central Europe	SEVIRI	SSMIS-MHS	Atmospheric River
3	12-13/09/2010	Europe	SEVIRI	SSMIS-MHS	PV anomaly
4	18/08/2012	Atlantic Ocean	SEVIRI	SSMIS-MHS	Atmospheric River
5	19/11/2009	Africa	SEVIRI	SSMIS-MHS	Atmospheric River
6	20/02/2010	Atlantic Ocean	SEVIRI	SSMIS-MHS	Atmospheric River

Outline

- **GAMES project**
- **GAMES rationale and objectives**
- **Task 1. Landmark target methodology**
  - Searching for ICI surface landmark targets
  - Results of ICI geolocation assessment
- **Task 2. Atmospheric target approach**
  - ICI absolute geolocation using DCC and WVM
  - ICI relative geolocation using BG approach
- **Task 3. Geolocation algorithm implementation**
- **Conclusion**

Task 2. Absolute geolocation using DCC

Absolute geolocation criterion:

comparison of existing PMW 183 GHz LEO imagery with Thermal InfraRed (TIR) GEO MSG satellite data pattern for deep convective precipitating clouds

Deep Convective Clouds (DCC)

ISSUES

- The contour matching is difficult to use, SEVIRI and PMW are not always consistent with each other for DCC (low correlations between TIR and MW).
- Different view geometry of SEVIRI and PMW is not obvious and might introduce relevant errors (parallax and distortion) depending on Cloud Top Height (CTH).
- CTH knowledge is limited for convective cores (especially for overshooting tops) that are not in thermal equilibrium. A CTH retrieval specialized for DCC using TIR and NWP forecast profiles has been developed,
- Errors due to view geometry are difficult to adequately compensate for, and these errors can strongly deteriorate the final result.

Task 2. Detection of DCC from MW and IR data

MW

Hong et al 2004

$\Delta T_{17} > \Delta T_{13} > \Delta T_{37} > 0$ K

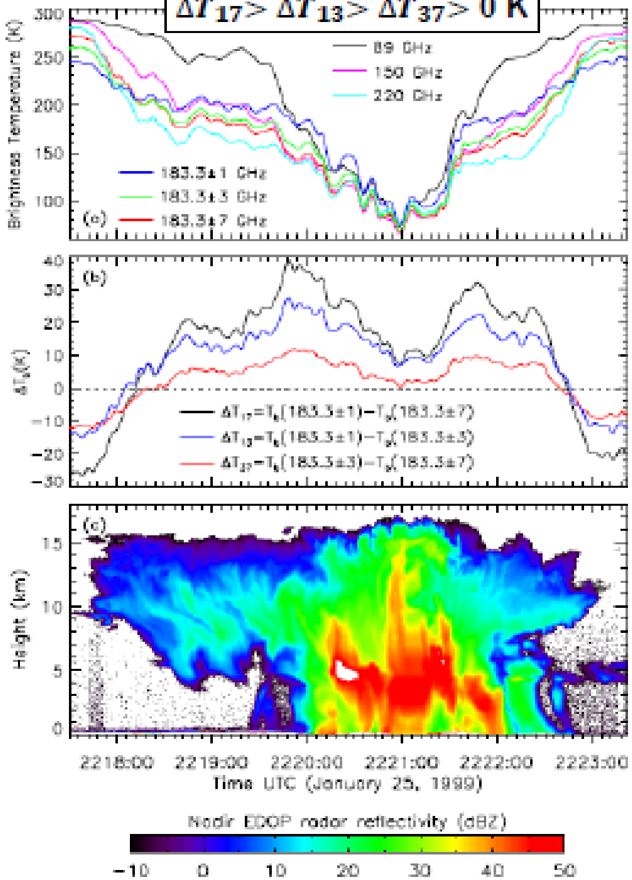

IR

Simplified method for Area selection:

TB 10.8 µm < 215

Bedka (2010), Brunner et al. (2007)

Task 2. MW and IR region-of-interest selection DCC

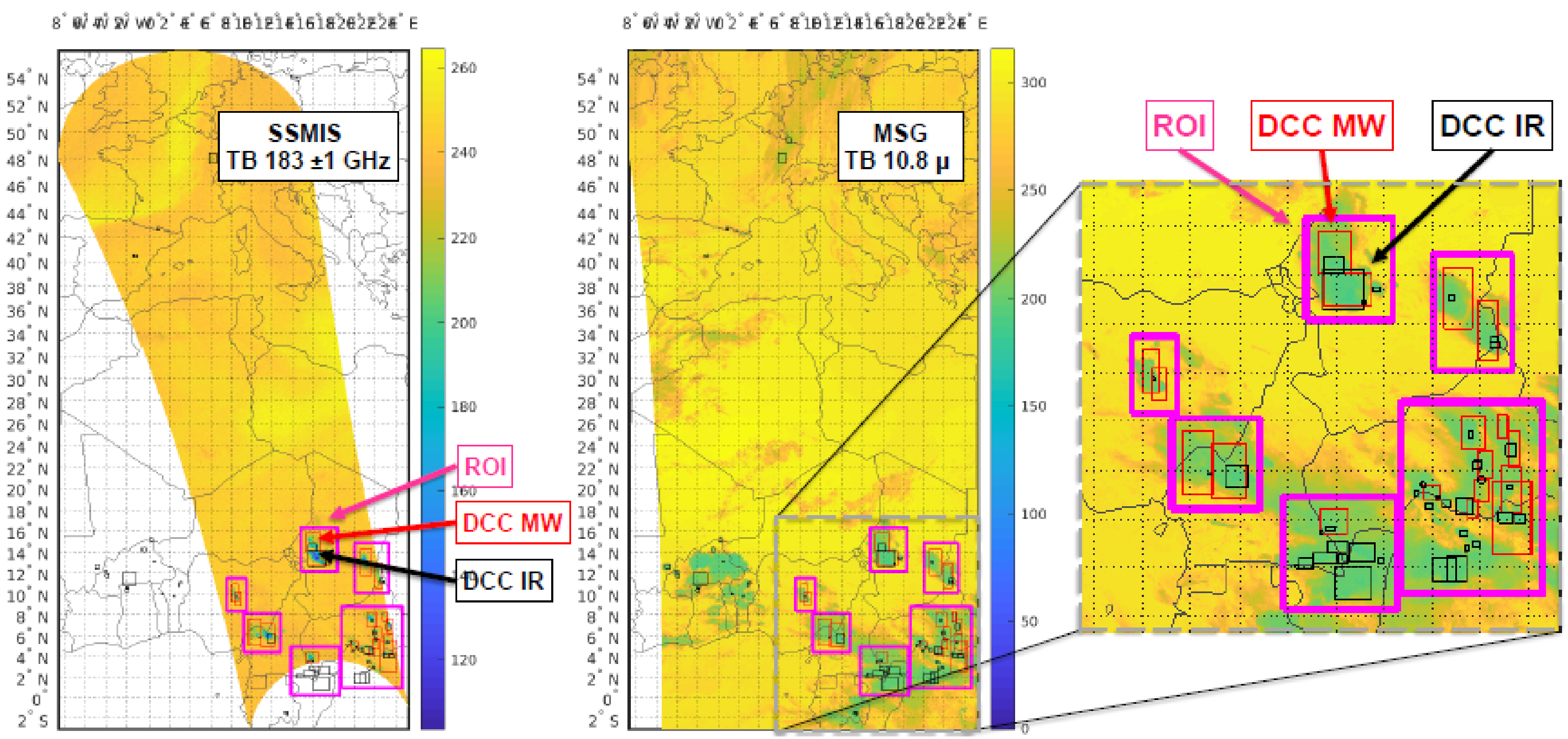

Task 2. Parallax correction for DCC flowchart

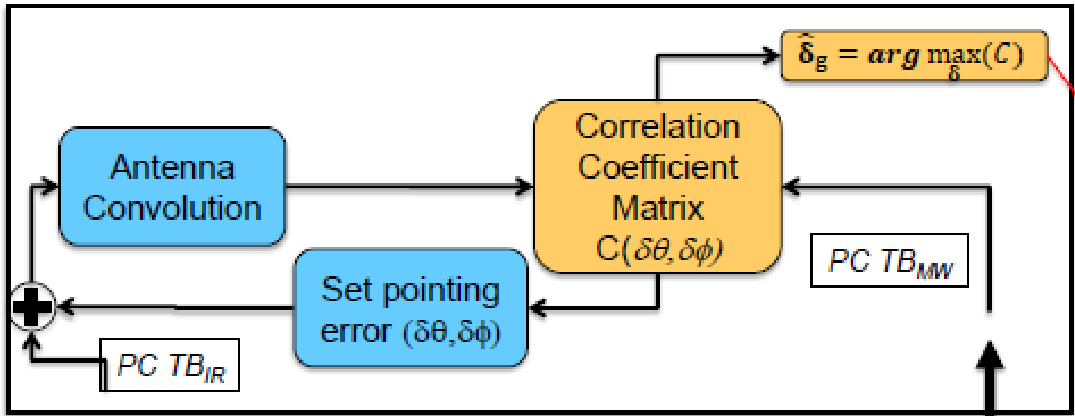

Correlation Coefficient Matrix is calculated direclty without using Fourier Transform (Masked Data)

20 steps of 0.02° in N-S E-W directions
Than 20 steps of 0.002° around *argmax(C)*

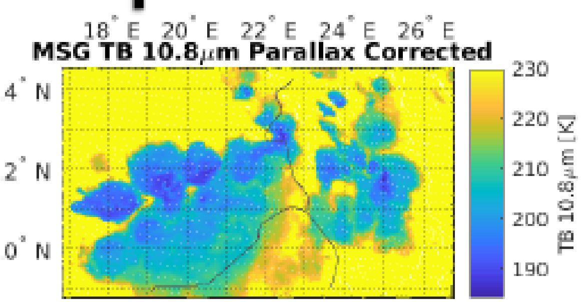

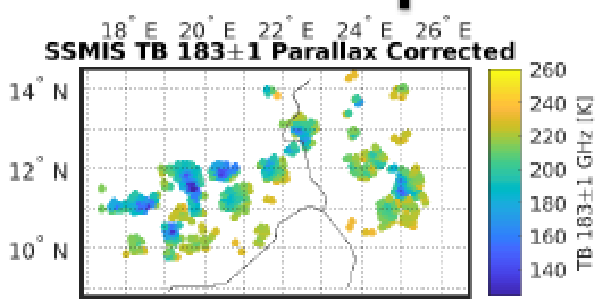

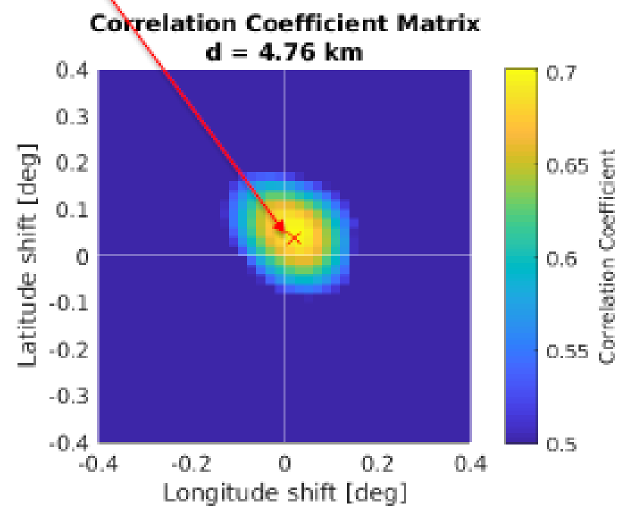

Task 2. DCC algorithm flowchart

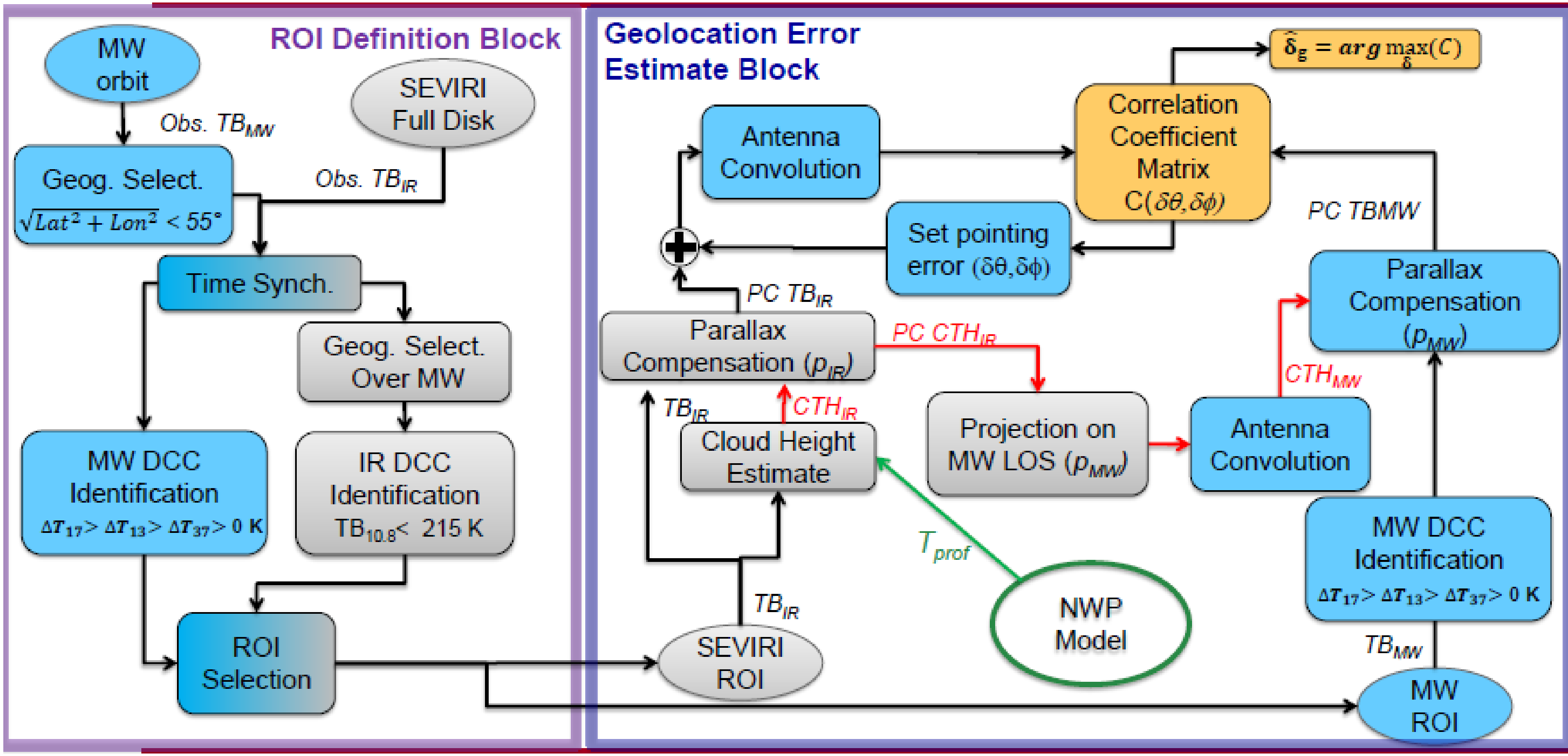

Task 2. Summary on DCC absolute geolocation

Absolute geolocation criterion:

comparison of existing PMW 183 GHz LEO imagery with Thermal InfraRed (TIR) GEO MSG satellite data pattern for deep convective precipitating clouds

Deep Convective Clouds (DCC)

- **Cloud Top Height Uncertainties**:
  1. We assumed no water vapor absorption over the cloud
  2. And an IR cloud emissivity = 1
  3. Temperature profile input has its own errors
  4. During the updraft phase (OT or not), the cloud is not in thermal equilibrium with the environment
  5. Lapse rate 8 K/km for overshooting tops is an average value

- **Relation between thermal IR and MW**:
  Thermal IR is sensible to CTH and mean radius at cloud top
  183 GHz MW to scattering from dense and high ice

  1. The correlation between IR and MW is usually weak
  2. Presence of cirrus clouds (or plumes) over the Deep Convective Cloud may further de-correlate them
  3. Extreme events with very strong and long lasting updrafts follow a different T-Tb_{ir} relation

Achieved error average is of the order of 5.3 km and the RMSE is of the order of 11.0 km.

Days	Orbits in MSG FD area	Num. of SSMIS segments	N total ROI	N Good ROI	Erro Mean Distance km	Erro Std Distance km	Mean correlation
17	180	203	170	109	9,7	5,33	0.71

Task 2. Issues on absolute geolocation using WVM

Absolute geolocation criterion:

comparison of existing PMW 183-GHz LEO imagery with Water-Vapor InfraRed (WVIR) GEO MSG satellite data pattern due to atmospheric humidity gradients (e.g., atmospheric WV rivers or stratospheric intrusions)

Water Vapor Masses (WVM)

Showing a coastal-like pattern with a pronounced gradient in both MSG and PMW signatures.

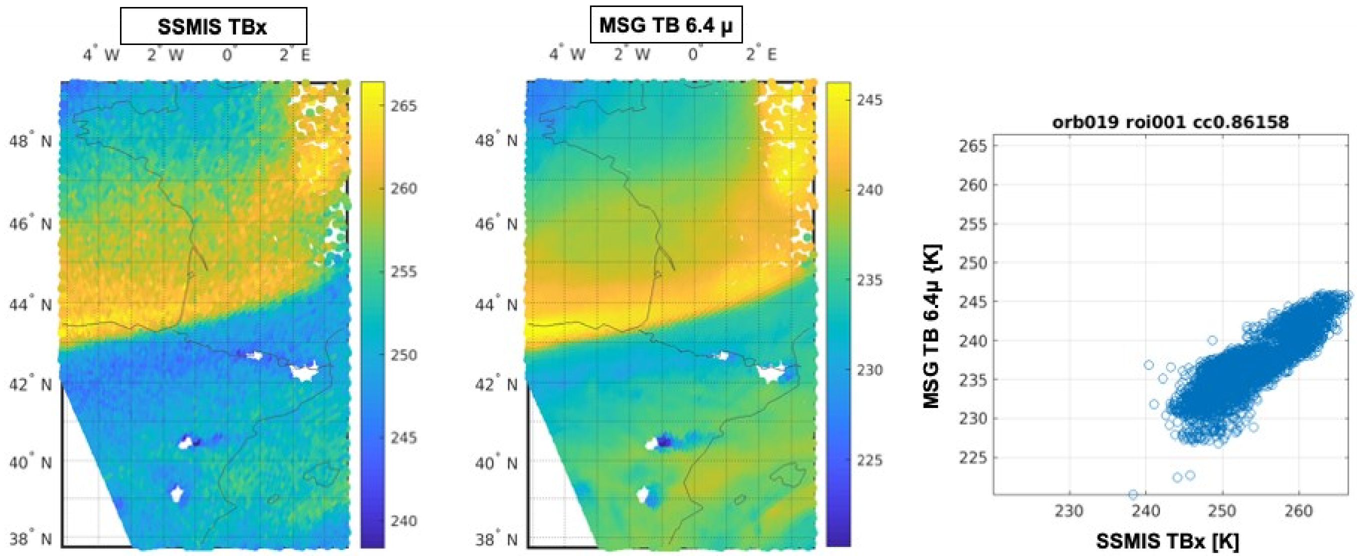

Absolute geolocation (Comparison of existing PMW 183 GHz with IR MSG)

Water Vapor Masses (WVM).

- Shows a coastal-like pattern with a pronounced gradient in both MSG and PMW signatures.
- Linear combination of weighting functions (WF) of PMW seems to be consistent with that of MSG-SEVIRI WV 6.2 µm thus facilitating the agreement between the two sources.
- For the quantitative analysis we used an average SSMIS TBx=1/2*[TB(183±1)+TB(183±3)]
- In terms of ICI WF those at ICI-8: 448±7.2 , ICI-7: 325±1.5 and ICI-11: 664±4.2 seems to be consistent with SEVIRI WV 6.2 µm.

Standard mid-latitude summer Nadir

SSMIS standard mid-latitude Summer 53.2°

ICI standard mid-latitude Summer 53.1°

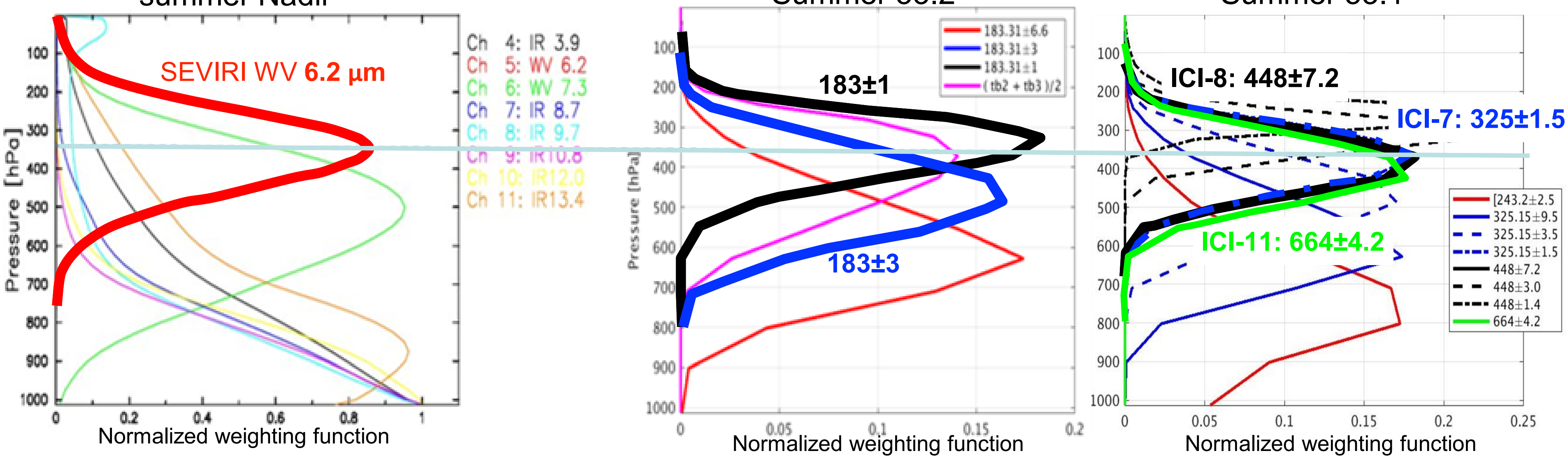

Task 2. WVM flow diagram

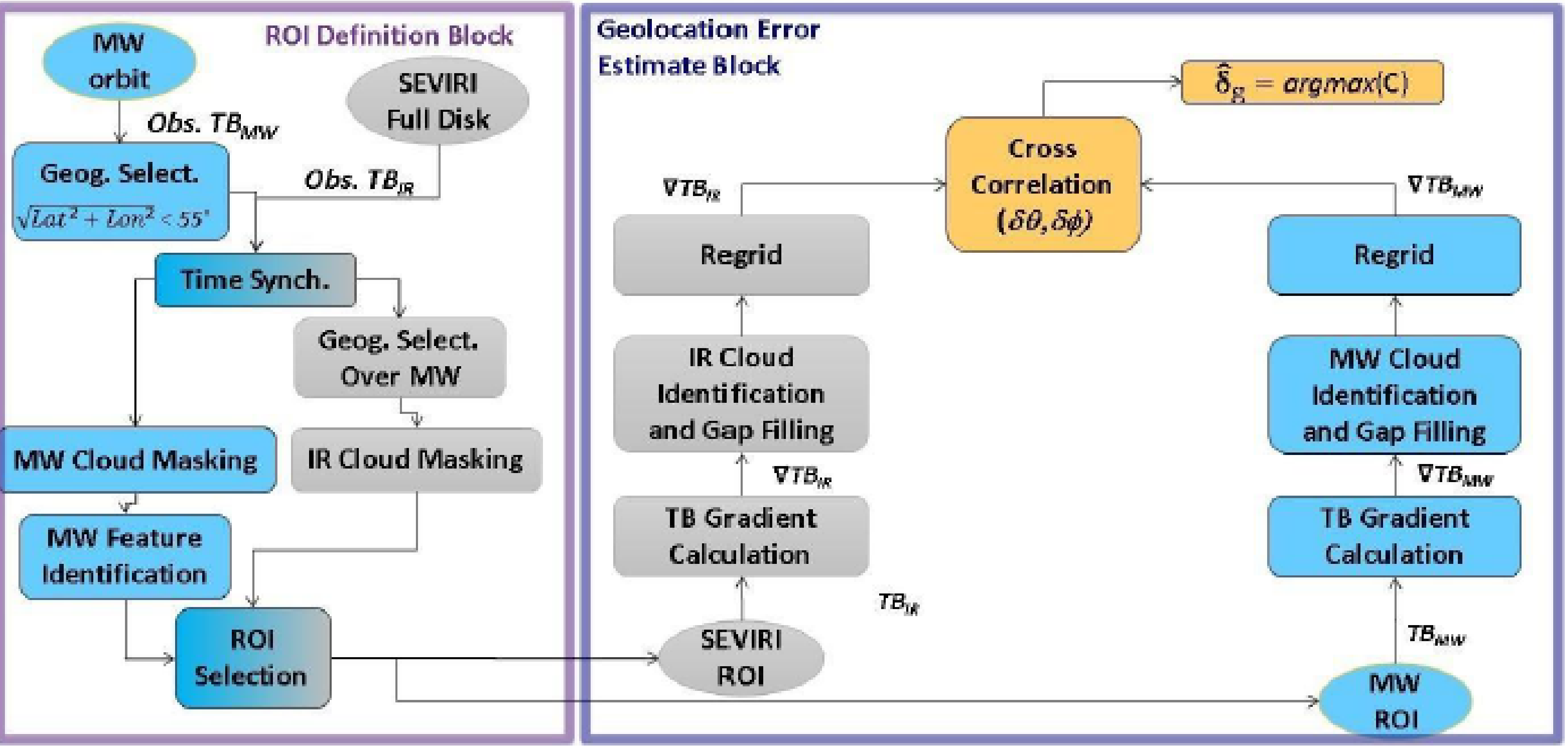

Task 2. WVM region of interest detection

MW Cloud masking:

$TB_{183\pm3} - TB_{183\pm1} < 10\ K$

IR Cloud masking:

$TB_{10.8} < 260\ K$

MW Feature Identification:

$$|\nabla(TBx)|^2 > 100$$

$$TBx = {}^{1}/_{2}\,(TB_{183\pm3} + TB_{183\pm1})$$

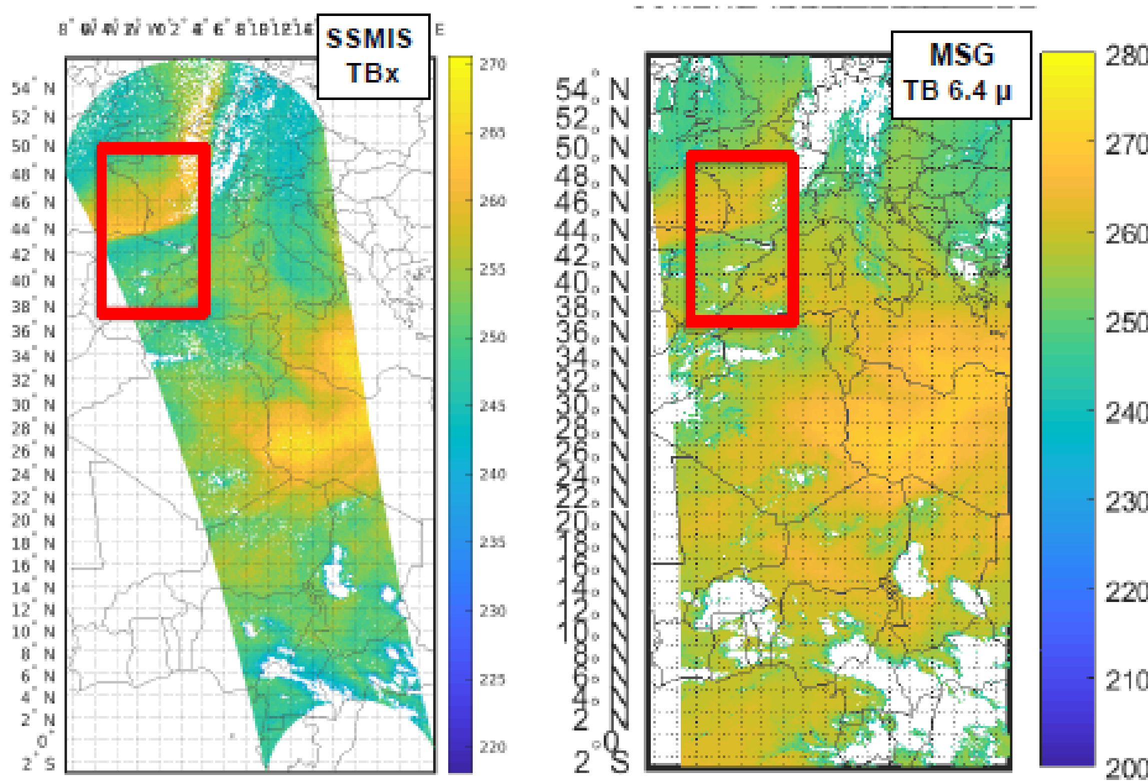

Task 2. IR-MW BT spatial correlation

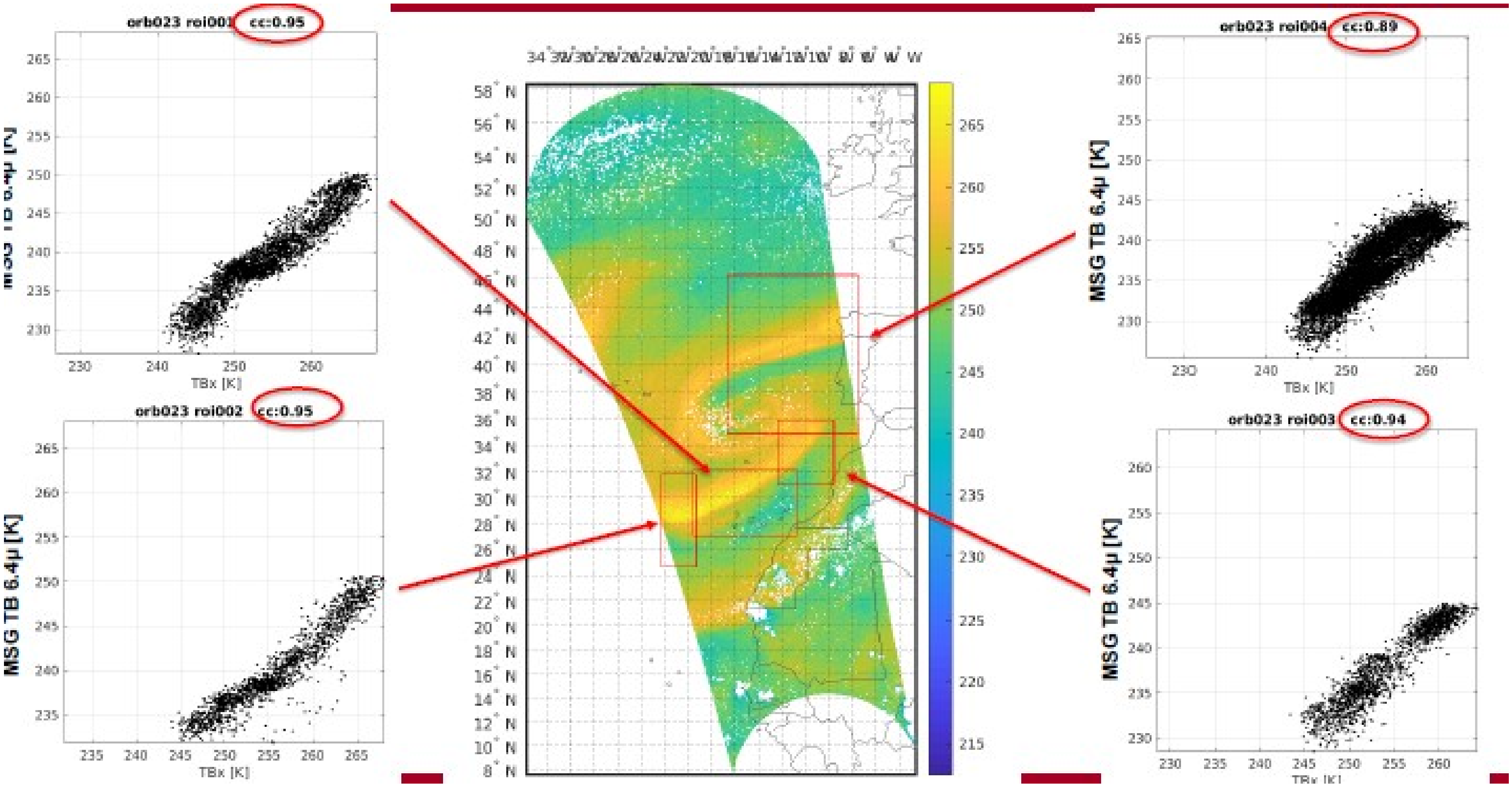

Task 2. Summary for WVM absolute geolocation

Absolute geolocation (Comparison of existing PMW 183 GHz with IR MSG) Water Vapor Masses (WVM).

- WVM shows a coastal-like pattern with a pronounced gradient in both MSG and PMW signatures (For the quantitative analysis we used an average SSMIS TBx=1/2*[TB(183±1)+TB(183±3)]).
- Linear combination of weighting functions (WF) of PMW seems to be consistent with that of MSG-SEVIRI WV 6.2 μm
- In terms of ICI WF those at ICI-8: 448±7.2 , ICI-7: 325±1.5 and ICI-11: 664±4.2 seems to be consistent with SEVIRI WV 6.2 μm.
- When considering the correlation between MSG and PMW of detected WVM in terms of its spatial gradient, for a long period of three months, the estimated PMW geolocation error standard deviation is of the order of 3.6 km and the RMSE is of the order of 5 km.

N Days	Orbits in MSG FD area	N SSMIS segments	N Total ROI	N Good ROI	Error Mean Distance km	Error Std Distance km	Mean correlation
17	180	203	152	35	3.30	3.72	0.63
90	969	2871	591	95	**3.64**	**3.60**	0.66

Conclusions on Task 2 ICI absolute geolocation

- DCC Drawbacks:
  - Is more complex algorithm
  - Has a lower accuracy with respect to landmark
- WV Drawbacks:
  - Low number of usable targets
  - Has a lower accuracy with respect to landmark (but higher than DCC)
- DCC Advantage:
  - High occurrence of targets
  - In areas without landmarks
  - Targets with strong contrast in MW
- WV Advantage:
  - Is less complex algorithm
  - In areas without landmarks
  - Targets often with simple coast-like shape

Target	Detectability/day	Discarded samples [percentage]	Geolocation accuracy average [km]	Geolocation accuracy standard deviation [km]
Deep Convective Clouds	10 (MSG only)	35.9 %	9,7	5,33
Water Vapor Features	7-8 (MSG only)	77-84 %	3.13	3.69

Outline

- **GAMES project**
- **GAMES rationale and objectives**
- **Task 1. Landmark target methodology**
  - Searching for ICI surface landmark targets
  - Results of ICI geolocation assessment
- **Task 2. Atmospheric target approach**
  - ICI absolute geolocation using DCC and WVM
  - ICI relative geolocation using BG approach
- **Task 3. Geolocation algorithm implementation**
- **Conclusion**

Task 2. Goal of the relative Geolocation

- **Goal: estimate the FOVs geolocation errors for each ICI-*i*ch wrt. ICI-rf**
- **Assume a reference (rf) ch. perfectly geolocated ICI-rf (e.g. using land marks)**
- **Since ICI nominal FOVs point differently a FOV remapping is considered.**

  >> ICI-*i*ch remapped onto ICI-rf

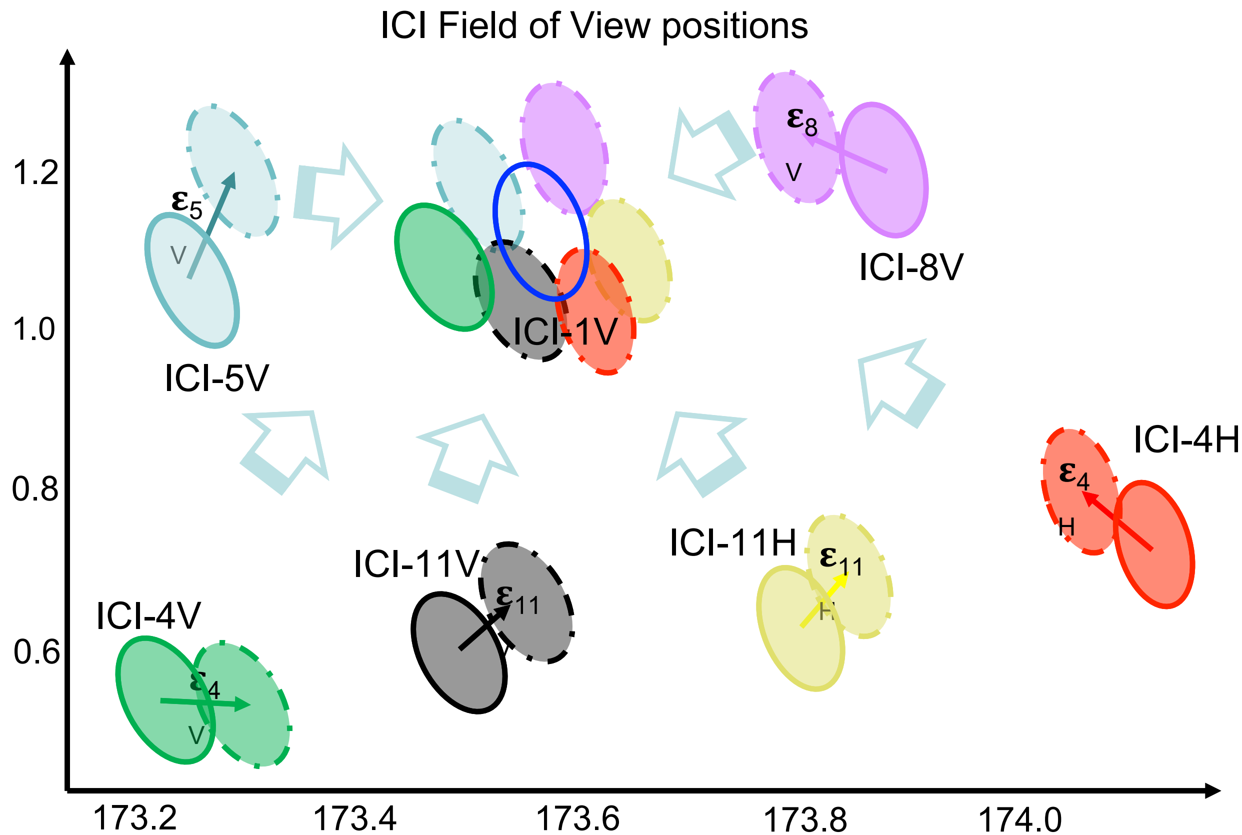

SAPIENZA UNIVERSITÀ DI ROMA

MolFloW

Task 2. Simulated dataset for ICI geolocation

- **Simulations are provided by MolFlow** (tech. Report TR/BG/MWI-ICI Issue 1.0, Rev. 1)
- **ERA5 INPUT fields**
  - Horizontal resolution (0.25° about 30 km)
  - Vertical resolution variable up to an altitude of 80 km
  - Time sampling 1 hour
  - Data considered (Metop-A orbits)
    - orbit **4655** and **4656**: from 08:00 to 13:00 UTC from forecast@2007-09-12T06:00:00
    - orbit **6985**: from 08:00 to 11:00 UTC from forecast @2008-02-23T06:00:00
    - orbit **9744**: from 13:00 to 16:00 UTC from forecast @2008-09-04T06:00:00
- **T_B OUTPUT fields**
  - **MWI/ICI sensor's characteristics considered**
  - **Four orbit considered**
    - Orbit 4655 on 2007-Sept-12 from 08:43:03 to 2007-Sept-12 10:22:03
    - Orbit 4656 on 2007-Sept-12 10:22:03 to 2007-Sept-12 12:04:03
    - Orbit 6985 on 2008-Feb-23 08:46:03 to 2008-Feb-23 10:28:03
    - Orbit 9744 on 2008-Sept-04 13:37:26 to 2008-Sept-04 15:16:22
  - **Core calculations are performed by ARTS v2.3.x (Buehler et al., 2018)**

The simulated dataset is used to verify Deep convective clouds (DCC) and atmospheric rivers (AR) features observable from MWI / ICI and to verify if the spatial remapping among channels (Bakus Gilbert) and cross correlation can be used to detects some geolocation errors.

SAPIENZA UNIVERSITÀ DI ROMA

Task 2. Simulated dataset for DCC

- **8 cases of DCC were selected**
- **Ice water path (IWP) is used to drive the case selection.**

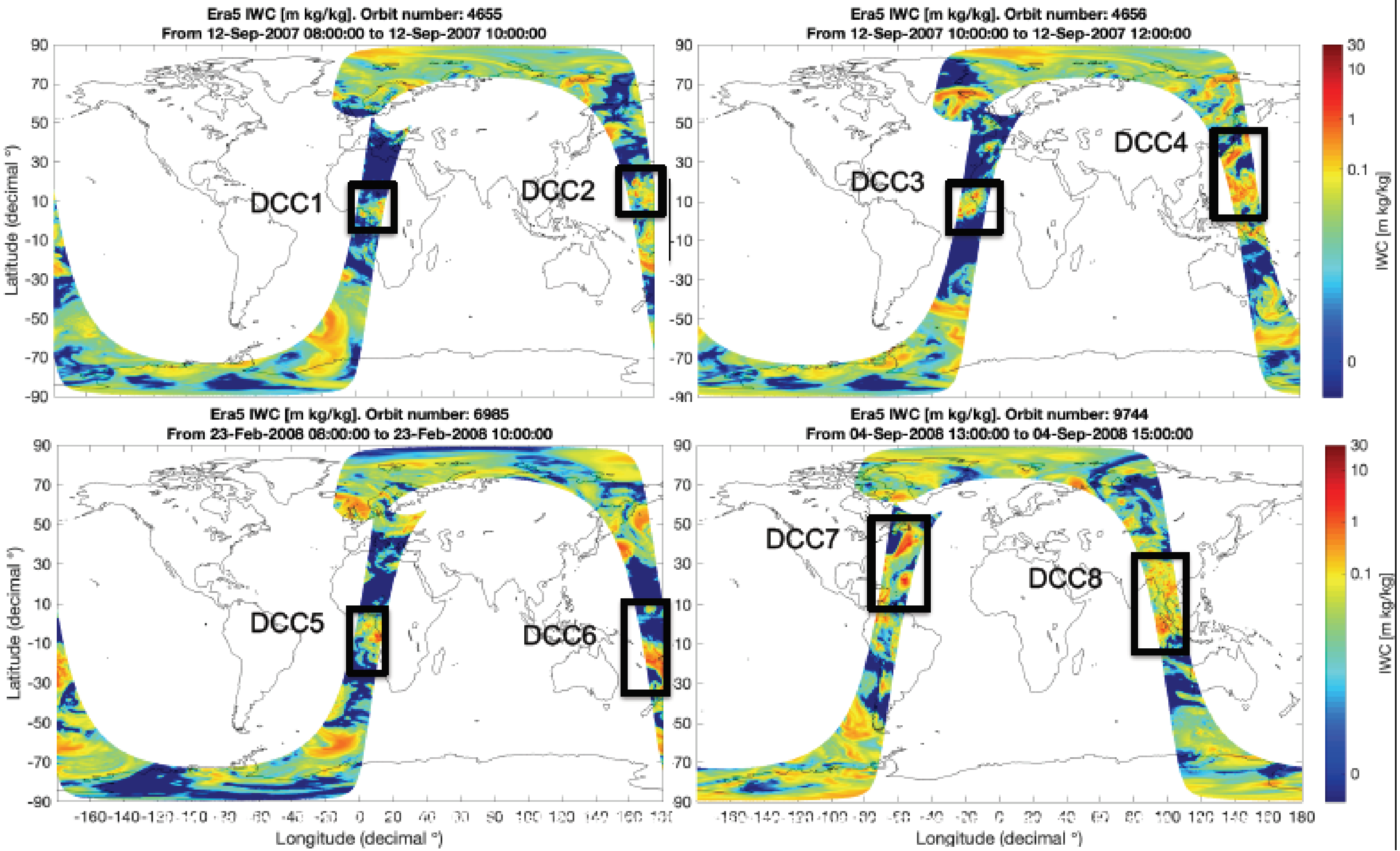

algorithm in [10]

Task 2. Open Loop Correlation (OLC)

Relative geolocation - Open Loop Correlation (OLC)

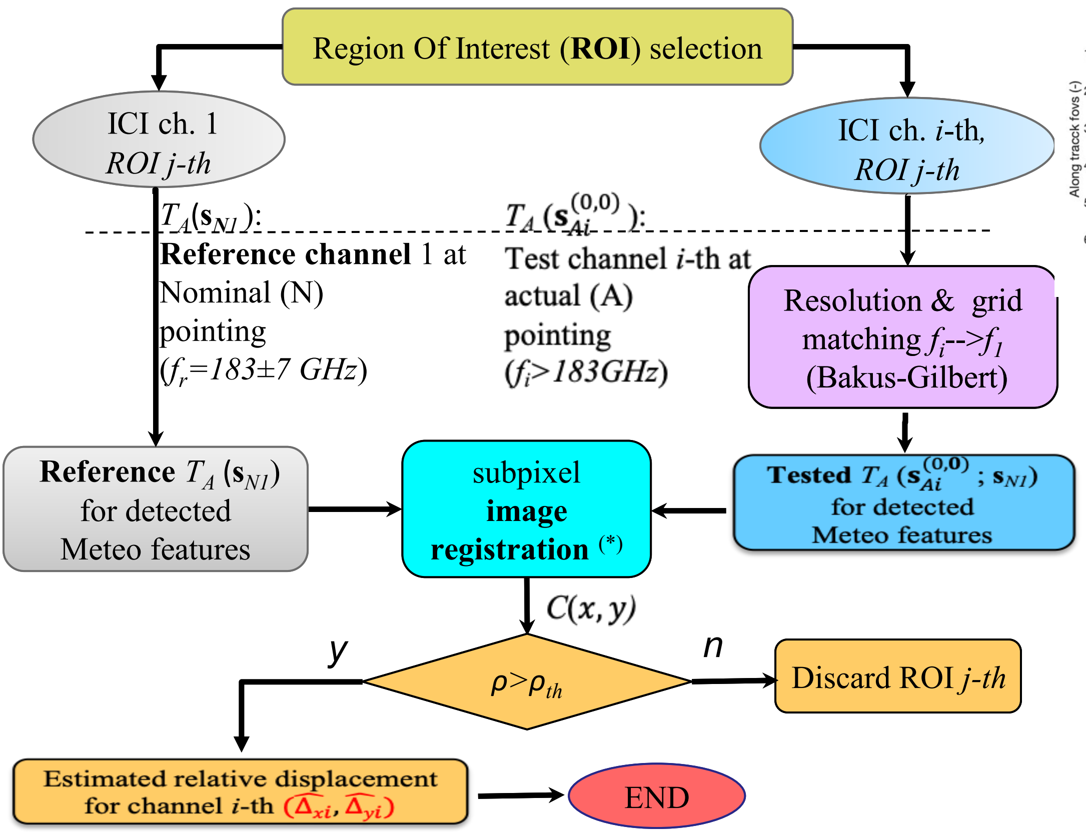

Automatic ROI selection

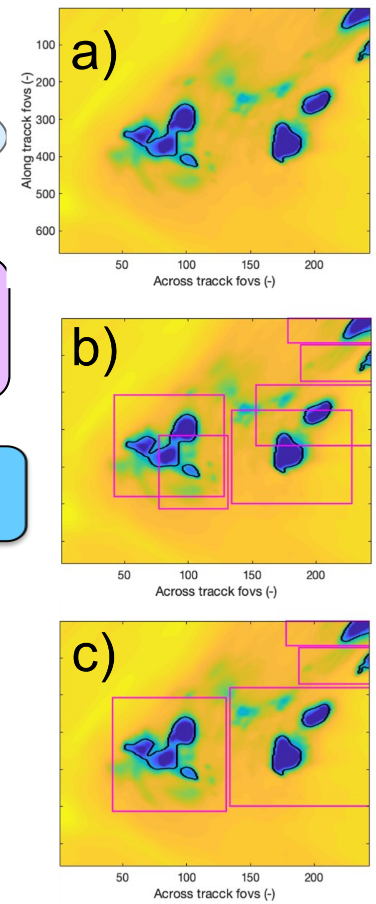

Identification rule:

$$\Delta T_{Aij} = T_A(183 \pm i) - T_A(183 \pm j)$$

$$\Delta TA_{31} > \Delta TA_{32} > \Delta TA_{21} > 0$$

Box bounding of identified ROIs

Grouping of overlapping boxes and enlarging them

(*) Manuel Guizar-Sicairos, Samuel T. Thurman, and James R. Fienup, "Efficient subpixel image registration algorithms," Opt. Lett. **33**, 156-158 (2008) . Matlab implementation “dftregistration.m” from file exchange. Copyright (c) 2016, Manuel Guizar Sicairos, James R. Fienup, University of Rochester. All rights reserved.

Task 2. ICI relative pointing error results

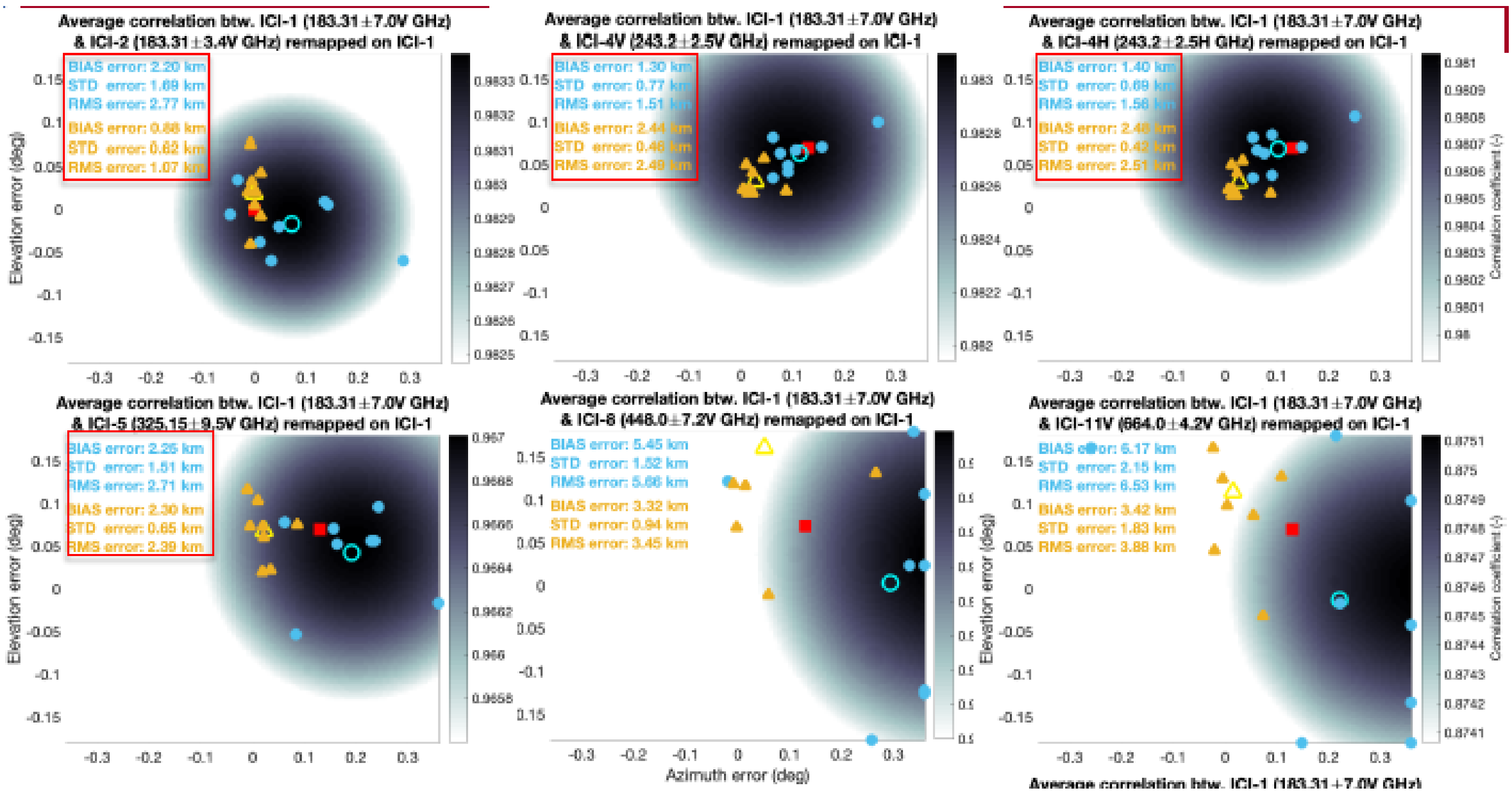

Task 2. ICI channel relative geolocation - Results

- **Deep convective clouds targets**
- **Backus-Gilbert used to remap FOVs from ICI-ith to ICI-1V or ICI-4V**

	TEST CASE A				TEST CASE B			
	Manually identified ROIs as in figure 5.4.2 (8 ROIs are considered)				Automatically identified ROIs as in section 5.6.3 (all detected ROIs are considered)			
REF vs. TEST	BIAS	STD	RMSE	N ROIs	BIAS	STD	RMSE	N ROIs
ICI-1 vs. ICI-2	0.88	0.62	1.07	8	1.07	0.70	1.28	18
ICI-1 vs. ICI-4V	2.44	0.46	2.49	8	2.41	0.57	2.48	18
ICI-1 vs. ICI-4H	2.48	0.42	2.51	8	2.44	0.55	2.50	18
ICI-1 vs. ICI-5	2.30	0.65	2.39	8	2.48	0.70	2.58	18
ICI-1 vs. ICI-8	3.32	0.94	3.45	8	4.92	3.15	4.40	16
ICI-1 vs. ICI-11V	3.42	1.83	3.88	8	4.53	2.72	4.58	17
ICI-1 vs. ICI-11H	3.37	1.74	3.80	8	4.46	2.63	4.54	17

- Reference: ICI-1
Each ch. is mapped on ICI-1

- (ICI-4, ICI-5) Geolocation error (**RMSE~2.5 km**)
- (ICI-8, ICI-11) Geolocation error (**RMSE~4.5 km**)

	TEST CASE A				TEST CASE B			
	Manually identified ROIs as in figure 5.4.2 (8 ROIs are considered)				Automatically identified ROIs as in section 5.6.3 (all detected ROIs are considered)			
REF vs. TEST	BIAS	STD	RMSE	N ROIs	BIAS	STD	RMSE	N ROIs
ICI-4V vs. ICI-2	2.71	0.46	2.75	8	2.91	0.61	2.97	18
ICI-4V vs. ICI-4V	0.00	0.00	0.00	8	0.00	0.00	0.00	18
ICI-4V vs. ICI-4H	0.06	0.03	0.07	8	0.10	0.13	0.16	18
ICI-4V vs. ICI-5	1.01	0.44	1.10	8	0.95	0.83	1.27	18
ICI-4V vs. ICI-8	3.46	1.81	3.90	8	3.29	2.54	4.15	17
ICI-4V vs. ICI-11V	2.65	1.02	2.84	8	2.92	2.44	3.81	18
ICI-4V vs. ICI-11H	2.54	0.98	2.72	8	2.84	2.37	3.70	18

- Reference: ICI-4V
Each ch. is mapped on ICI-1

ICI-5 RMSE improved by a factor 2
ICI-11 RMSE improved by a factor 1.2
ICI-8 RMSE unchanged
ICI-2 RMSE worsened by a factor 2.3

Task 2. ICI channel relative geolocation - Comment

- **Why reference ICI-4V performs better than ICI-1V?**
  - ICI-4V better correlates with the other ICI tested channels
  - Avg. Corr (ICI-4 vs. ICI-11) =0.91
  - Avg. Corr (ICI-1 vs. ICI-11) =0.88

This could help explaining the additional 0.8km in the pointing errors for ICI-11 if considering reference ICI-1 than ICI-4.

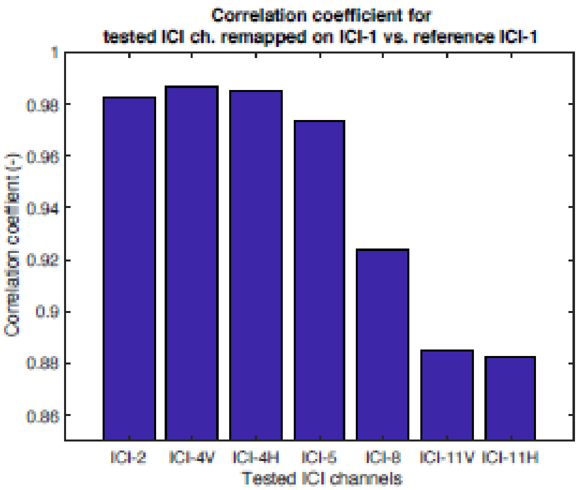

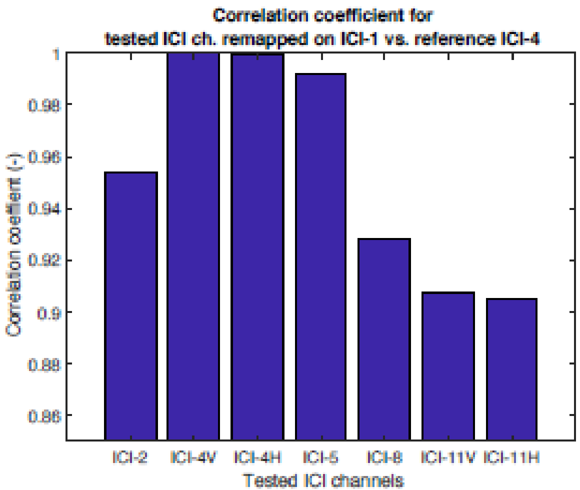

Figure 6.7.2: correlation coefficient between tested and ICI-1 (left) and ICI-4V (right) reference channel

➢ The worse performance obtained for ICI-8 and ICI-11 with respect to ICI-4 and ICI-5 could be related to the differences in the information content in the TB observations of these two sets of channels.
Qualitatively, this is quite evident in the images of simulated DCC events where the T_B depression due to the scattering by the ice in the convective cloud has a different pattern, i.e. clouds are more smeared, for ICI-11 than ICI-4, for example.

Conclusions on Task 2 and recommendations

- **ICI channel absolute geolocation**
  - **Water Vapor Masses (VWM)** features as seen by ICI-2 and ICI-3-like SSMIS channels and MSG SEVIRI water vapor 6.3 µm channel, have demonstrated to be a good candidate **atmospheric target** to be used for an absolute geolocation of ICI-2 and ICI-3.
  - The achieved geolocation errors are comparable, in terms of RMSE, with those obtained from the landmark approach.
  - For a future implementation we suggest to accurately take the WVM approach into consideration at least as an optional off-line tool even operated by third parties.

- **ICI channel relative geolocation**
  - Assuming ICI-4 as reference channel in the OLC, we expect to achieve relative geolocation **errors less than 4.1 km for all the ICI ch.s**
  - ICI-2 results to be less correlated with ICI-4 than ICI-1.
  - The relative geolocation of ICI-1, ICI-2 and ICI-3 could be less accurate and an absolute geolocation approach (e.g. using landmarks or water vapor masses features) could be a safer option.

Outline

- **GAMES project**
- **GAMES rationale and objectives**
- **Task 1. Landmark target methodology**
  - Searching for ICI surface landmark targets
  - Results of ICI geolocation assessment
- **Task 2. Atmospheric target approach**
  - ICI absolute geolocation using DCC and WVM
  - ICI relative geolocation using BG approach
- **Task 3. Geolocation algorithm implementation**
- **Conclusion**

Task 3. GAMES geolocation validation prototype tool

A **GAMES toolbox for geolocation validation** of imager data following methods described in Task 1 and 2 have been implemented in a Python package called *games*, that contains four methods/pipelines named:

- gtopo30: mountain chain as target reference
- sar: ice shelf or water way as target reference
- gshhg: boundary between lake and land as reference
- rpe: relative pointing error (Open Loop Correlation)

for validating ICI, MWI, and SSMIS data using various type of reference data

games is portable:

the package includes a build script, that builds a *games* Docker image, that is portable, and *games* pipelines can run inside *a Docker* container on machines that have a Docker engine installed

- a Docker image is a non-changeable file containing libraries, source code, tools and other files needed to run applications.
- a Docker Container is the run time instance of the image, and data files can be mounted into this container

games has a CLI (command line interface):

see examples on next slide

games is modular:

The package contains 22 source code files or modules with well separated responsibilities, and games can be used as a "normal" python package if desirable

The packages includes unit tests (and a setup for running these) on all functions and methods of classes defined in the various modules, that will facilitate for further developments

Deliverable document 08 – D08

Algorithm Theoretical Baseline Document

Task 3. GAMES pipeline for absolute geoloc.

Name of pipeline	Type of target	Target members
gshhg	lake at high altitude or coast-line at high latitude	Qinghai Lake, Titicaca Lake, and Hudson Bay
gtopo30	mountains area	Andean Mountains and Karakorum mountains
sar	ice shelf and waterway	Ross Antarctic ice shelf, Filchner-Ronne Antarctic ice shelf, Amery Antarctic ice shelf, and Nares Strait
rpe	deep convective clouds	N/A

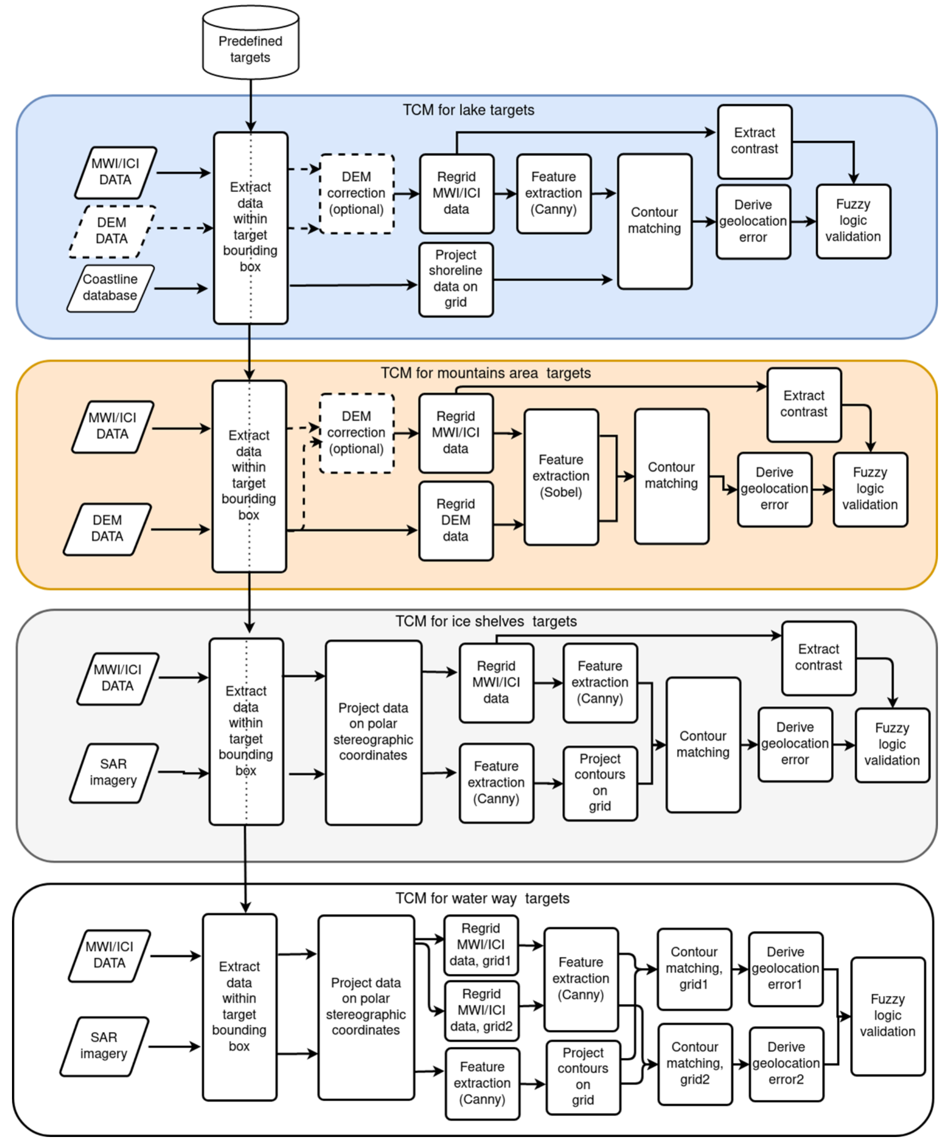

Task 3. GAMES data flow for relative geoloc.

High level description of data flow of the “relative pointing error” pipeline

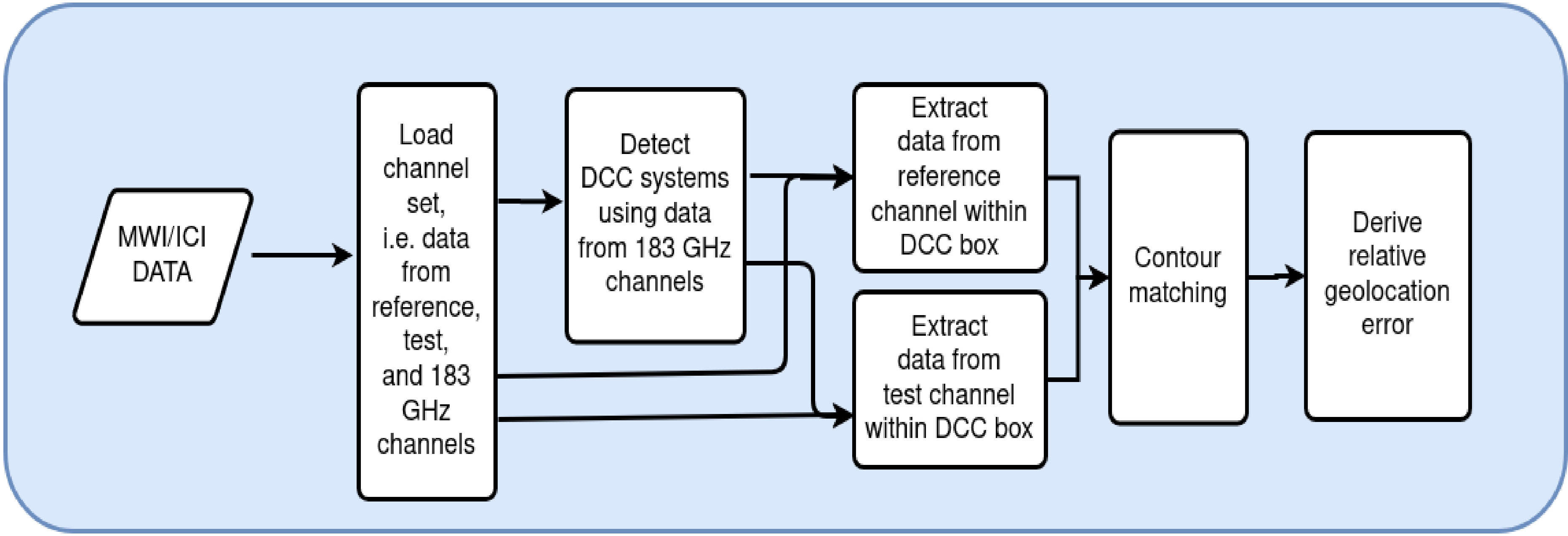

Task III – Running GAMES prototype tool

Example how to run games (CLI of games)

Running the container to see what "pipelines/services" or validation methods that are available:

```
$ docker run --rm molflow/games --help

usage: games.sh [-h] {gtopo30,sar,gshhg,rpe}

Games Admin

positional arguments:
  {gtopo30,sar,gshhg,rpe}
                        The service to run. For more help on a particular
                        service do `SERVICE --help`

optional arguments:
  -h, --help            show this help message and exit
```

The obtained **result** from processing the data **is written** to a **netcdf file** (in the **OUTDIR** directory)

```
$ GSHHG="/your/local/path/to/gshhg-shp-2.3.6/GSHHS_shp/"
$ GTOPO="/your/local/path/to/gtopodata/"
$ SSMIS="/your/local/path/to/smissdata/"
$ LEVEL1BFILE="CSU_SSMIS_FCDR_V01R01_F17_D20161221_S2348_E0130_R52279.nc"
$ OUTDIR="/your/local/path/to/result/"

$ docker run --rm -v $GSHHG:/gshhg -v $GTOPO:/gtopo -v $SSMIS:/level1b -o $OUTDIR:/outdir \
    molflow/games gshhg $LEVEL1BFILE qinghai --demcorrection  --storeresult
```

Task 3. Test dataset and verification

A test dataset covering one year (2016) of F-17 SSMIS and validation data has been collected and this is described in a Test Dataset document.

The total size of this data package is about 200 GB.
The dataset contains the following data:

For landmark targets:

- DEM - GTOPO30 - GTOPO30 is a global digital elevation model dataset that is divided into 33 tiles. The resolution is 30 arc seconds (~1 km). This data is used both for DEM correction of imager data and as reference data for mountains area targets
- Boundary between lake and land - GSHHG
- The Global Self-consistent, Hierarchical, High-resolution Geography Database (GSHHG) is a dataset that contains e.g. polygons with the
- Boundary between land and ocean and between land and lake.
- Boundary between ice shelf and ocean - SAR
- Level-1 GRD SAR data is used to obtain contours of ice shelf targets, and the dataset contains preprocessed data SSMIS F-17 (note that we have used data from the channel operating around 183±6.6 GHz in horizontal polarization, but the dataset contains data for more channels)

For atmospheric targets:

Remapped ICI data (simulated data covering four reference orbits)

Target contour matching (TCM) – Landmark targets

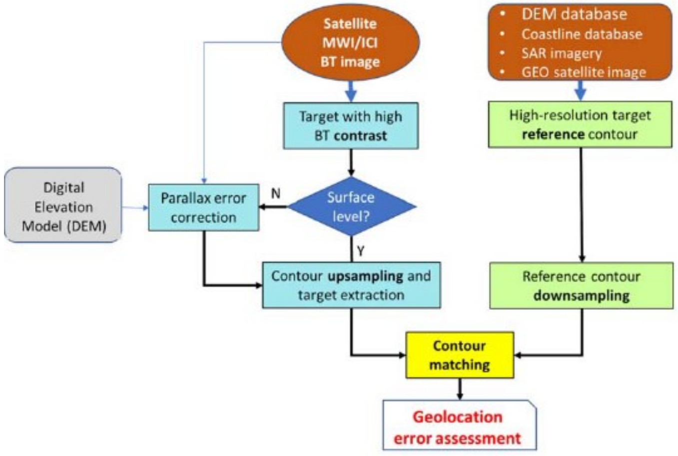

Task 3. Test dataset intercomparisons

The games toolbox has been used for processing the test dataset. Results have been **compared to the results obtained from the prototype code** used for producing data for Task 1 (landmark) and Task 2 (relative pointing error) report

Ex: Ice shelves

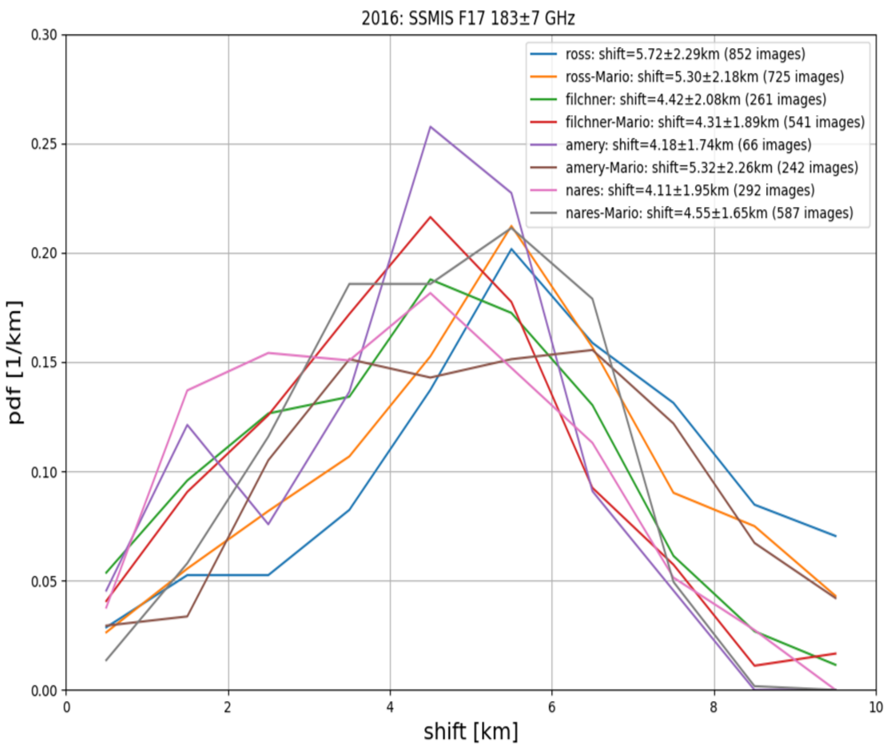

Ex: Mountain area targets

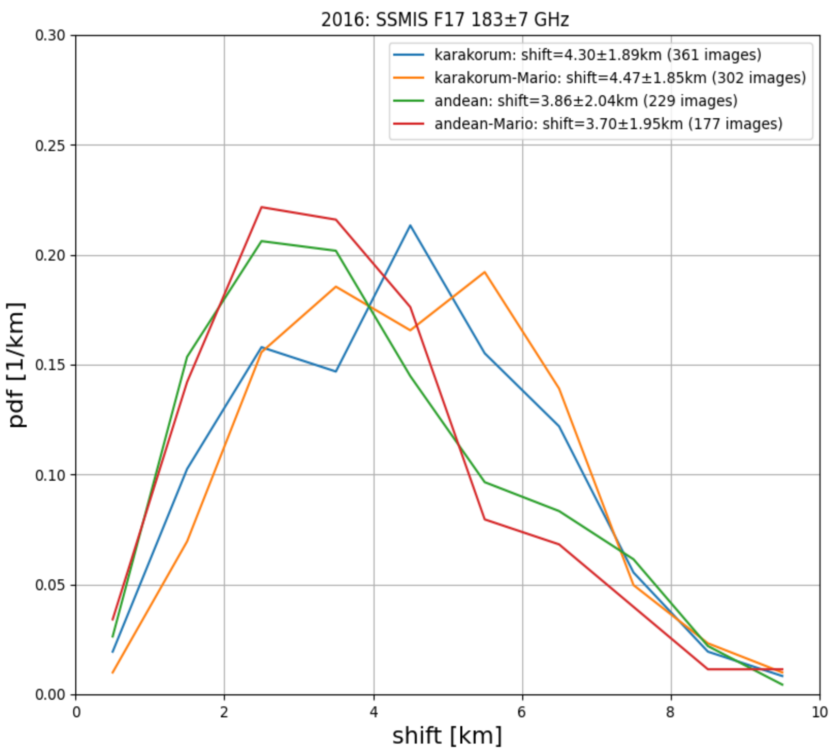

Task 3. Test dataset processing for RPE

Relative pointing error assessment algorithm

Testing **relative pointing algorithm and derived errors** for ICI Channels and from a simulated dataset.

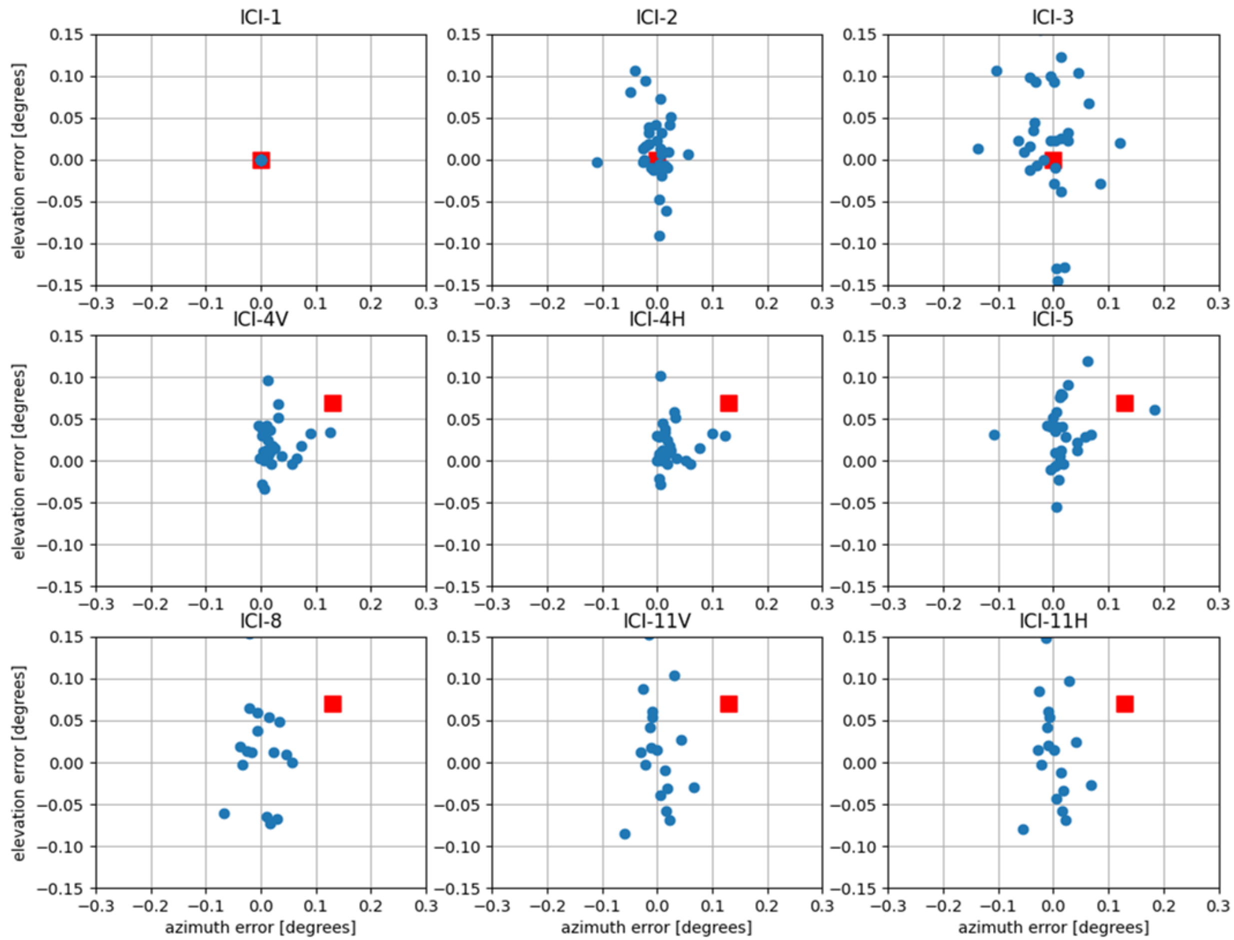

The **red marker** indicates the true pointing error of each channel, and the blue dots the derived error from 32 different bounding boxes that were identified to contain deep convective clouds.

The result is in good agreement to what is presented in Task 2 report.

Outline

- **GAMES project**
- **GAMES rationale and objectives**
- **Task 1. Landmark target methodology**
    - Searching for ICI surface landmark targets
    - Results of ICI geolocation assessment
- **Task 2. Atmospheric target approach**
    - ICI absolute geolocation using DCC and WVM
    - ICI relative geolocation using BG approach
- **Task 3. Geolocation algorithm implementation**
- **Conclusion**

GAMES overall conclusion

- The **GAMES project** has basically to achieve the objectives of all 3 tasks
- New and effective **landmark targets** have been searched and found, useful references to validate the geolocation error also for future mm-wave PMW missions:
  - *Antarctica ice shelves*
  - *High-altitude lakes (Qinghai and Titicaca)*
  - *Mountain slopes (Andes and Karakorum)*
  - *High-latitude straits (Nares) and bays (Hudson)*

    > Geolocation assessment error average (AVG) = about *4.8 km*

    > Geolocation assessment error standard deviation (STD) = about *2.1 km*
- Other approaches with **atmospheric targets** have been investigated:
  - Deep Convective Clouds (DCC): interesting, but not suitable in terms of accuracy
  - **Water Vapor Mass (WVM)** coupling WV-GEO data: attractive (AVG ≅ 3.6 km; <STD≅3.6 km)

    ⇒ complementary to landmark-target approach especially for target-free regions
- A **relative pointing error geolocation** assessment between ICI channels proposed
  - based on a Backus-Gilbert remapping approach
  - using as a reference ICI-1 with STD<3.1 and ICI-4 with STD<2.6 km
- The GAMES project has delivered to Eumetsat a ATBD and an **operational tool "games" in Python** useful for ICI CAL/VAL operational and commissioning activity.

… the ultimate finding.

Geolocation
Assessment
Methods for
Eumetsat Polar System
Second Generation ICI and MWI

Lockdown Poem

Locked in a house
Observing the sky
Cramped in your room
Keeping tidy
Drying clothes
Other than that
Well
Now where was I?

Trinity college, Manchester (UK), 8 years old student

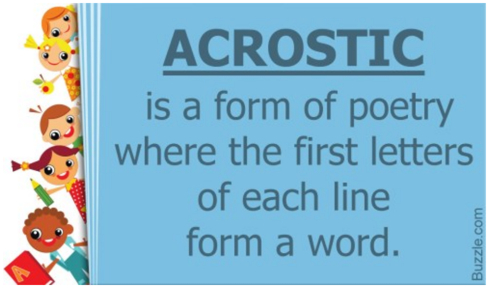

Thank you.
Contacts: frank.marzano@uniroma1.it